CNIC-01630
CNDC-0031
INDC(CPR)-056/L

COMMUNICATION OF NUCLEAR DATA PROGRESS

No. 26 (2001.12)

China Nuclear Data Center
China Nuclear Information Centre
China Nuclear Industry Audio & Visual Publishing House

COMMUNICATION OF NUCLEAR DATA PROGRESS

EDITORIAL NOTE

From last issue, the layout of CNDP has been changed to serve our reader better. The editors hope that our readers and colleagues will not spare their comments in order to improve this publication. If you have any, please contact us by following address:

Mailing Address: Profs. LIU Tingjin and ZHUANG Youxiang
China Nuclear Data Center
China Institute of Atomic Energy
P.O. Box 275 (41), Beijing 102413
People's Republic of China
Telephone: 86-10-69357729 or 69357830
Facsimile: 86-10-6935 7008
E-mail: tjliu @ iris.ciae.ac.cn or yxzhuang @ iris.ciae.ac.cn

Abstract: This is the 26th issue of *Communication of Nuclear Data Progress* (CNDP), in which the progress and achievements in nuclear data field from the last year up to now in China are carried. It includes the measurements of ^{71}Ga, ^{94}Zn, ^{191}Ir, ^{174}Hf(n,γ) and ^{114}Cd(n,2n) cross sections, fission product yields of n+$^{235,\ 238}$U, DPA cross section calculated with UNF code, fission barrier parameter evaluation of some nuclides, production and transmission of covarience in the evaluation processing of fission yield data and transmission analysis of Ne-line Ge XXIII.

Communication of Nuclear Data Progress

No.26 (2001) Beijing

CONTENTS

Measurement of Neutron Capture Cross Section of ^{174}Hf in The Energy Range from 162 to 1200 keV

XIA Yijun LUO Xiaobing YANG Zhihua

Institute of Nuclear Science and Technology, Sichuan University, Chengdu, 610064

【**abstract**】*The cross sections for the ^{174}Hf(n,γ)^{175}Hf reaction were measured relatively to the ^{197}Au(n,γ)^{198}Au reaction for neutron energies from162 to 1200 keV, using the activation technique with high resolution HPGE gamma ray spectroscopy. Some experimental data were given for the first time..*

Introduction

Natural Hf consists of six isotopes, i.e. ^{174}Hf(0.16%), ^{176}Hf(5.26%), ^{177}Hf (18.60%), ^{178}Hf (27.28%), ^{179}Hf (13.62%), and ^{180}Hf (35.08%). Before our work, there were no measurements on the cross sections for the ^{174}Hf(n,γ), ^{175}Hf reaction. In this work we measured the cross sections in the energy range from 162 to 1200 keV by the activation method.

1 Measurement

The samples are naturally metallic hafnium disks of 20 mm in diameter and 1.1mm in thickness. The gold disks of 20 mm in diameter and 0.1mm in thickness were used as the neutron fluence monitors. Each sample was sandwiched between two gold disks. The sample groups were wrapped in cadmium foils of 0.5 mm in thickness.

The irradiations were performed at 0 degree with respect to the incident proton beam. The neutrons of 164 keV were produced by the ^{7}Li(p,n) ^{7}Be reaction, and 469 to 1200 keV by the T(p,n)^{3}He reaction. The distance between the samples and the target was 10~15 mm. The proton beam currents were generally 8 to 12μA and the duration of irradiation was about 50 to 80 hours for each energy. The neutron fluence was monitored with a long counter at 0 degree at a distance of 1.8 m from the neutron source. In order to record the neutron fluence as a function of time during the irradiation, the integral count rate of the long counter per 5 minutes was recorded continuously by microcomputer multiscaler and stored in magnetic disk for correcting nonuniform irradiation history.

The activities of the samples and the gold disks were mersured with a calibreted high resolution HPGe detector. Because the activities of the samples were rather weak, they were placed on the surface of the detector for measurement. In order to obtain enough statistics for gamma ray counting, the time of activity measurement was about 45~50 hours for each sample. The relevant decay data of ^{175}Hf and ^{198}Au are listed in Table 1.

Table 1 Decay data of products

product nucleus	$T_{1/2}$	E_γ / keV	I_γ / %
^{175}Hf	70 d	343.4	84
^{198}Au	2.6935 d	411.8	95.5

2 Results

The cross sections for the ^{174}Hf(n,γ) ^{175}Hf reaction obtained with the standard cross section of ^{197}Au(n,γ)^{198}Au reaction taken from ENDF/ B-6 are listed in Table 2 .

Table 2 Measured cross sections

E_n / keV	σ / mb
162±21	459±28
469±83	294±18
683±110	231±16
789±112	226±16
997±102	217±15
1200±102	209±15

To our knowledge, no other experimental data have been found for the $^{174}Hf(n,\gamma)$ ^{175}Hf reaction up to now. These cross sections given by present measurements are the first experimental data. The main uncertainties came from the counting statistics in γ-activities, the standard cross section, the efficiency of γ-ray full energy peak, various corrections, ect.

Acknowledgment

The authors are indebted to China Nuclear Data Center for the financial support. We would like to thank the crew of 2.5 MV Van de Graaff Accelerator of Sichuan University.

Mass Distributions of 22.0 MeV Neutron-induced Fission of ^{238}U

LIU Yonghui YANG Yi FENG Jing BAO Jie LI Ze QI Bujia TANG Hongqing ZHOU Zuying
CUI Anzhi RUAN Xichao SUN Hongqing ZHANG Shengdong GUO Jingru

China Institute of Atomic Energy, P. O. Box 275(46), Beijing, 102413
e-mail yhliu@iris.ciae.ac.cn

【**abstract**】*Chain yields of 32 chains were determined for the fission of ^{238}U induced by 22.0 MeV mono-energetic neutrons for the first time. Fission product activities were measured by HPGe γ-ray spectrometry without chemical separation. Absolute fission rate was monitored with a double-fission chamber. The efficiency of the fission chamber was checked by determination of ^{198}Au activity from $^{197}Au(n,\gamma)$ ^{198}Au reaction[1].*

Introduction

The mass distributions in fission of ^{238}U has been extensively investigated, but only a few of those investigations deal with fission induced by mono-energetic neutrons. S. Nagy et al. Studied the mass distribution of ^{238}U with mono-energetic neutrons of 1.5, 2.0, 3.9, 5.5, 6.9, and 7.7 MeV [2]. Champman et al. determined the mass distribution for the fission of ^{238}U induced by neutrons with energies of 6.0, 7.1, 8.1, and 9.1 MeV[3]. Some of the determination of the fission product yields of ^{238}U induced by mono-energetic neutrons were also measured at CIAE. For instance, Li Ze et al. at 8.3 MeV neutrons [4], Zhang Chunhua et al. at 3.0 MeV neutrons[5], and Wang Xiuzhi et al. at 5.0 MeV neutrons[6]. And Su Shuxin et al. measured the mass distribution for the fission of ^{238}U with fission spectrum neutrons[7]. Several other measurements of the mass distribution are with 14MeV neutrons[8, 9]. In this work, measurements were carried out for the mass distribution of the fission of ^{238}U induced by 22.0 MeV neutrons, and 32 chain yields were obtained.

1 Experiment

The experiment was carried out at the HI-13 Tandem of CIAE. The tritium gas chamber was used to produce neutrons by the bombardment with the deuteron beam [10].

The neutron spectrum was measured with TOF technique in order to estimate the fission events by the low energy neutrons of energy between 0.8~8 MeV from D(d,np) ^{2}H and D(d,n) ^{3}He reaction, and from the scattering by environment. The ratio of low energy neutron fission events to 22.0 MeV neutron fission events was estimated. The samples used in the neutron irradiation were uranium metal disks of 1.6 cm diameter×0.05cm thickness with an average weight of about 1.5 g. The uranium disks were packaged in a pure aluminum foil of 0.2 mm thickness. The sample, which was sandwiched between standardized thin samples to monitor the fission rate absolutely, was mounted in double fission chamber. The efficiency of the fission chamber was checked by $^{197}Au(n,\gamma)$ ^{198}Au reaction with thermal neutrons. The standardized thin samples were made of the same natural uranium as the thick samples.

The double fission chamber was covered with cadmium of 1 mm thickness in order to shield it from the thermal neutrons from the environment. Four samples were irradiated for a period varying form 0.5 to 30 h at a distance of about 5 cm from the neutron source in the direction of zero degree.

After the irradiation, the samples were measured by a HPGe-92X Spectrum Master of γ-spectrometer. The resolution of the 120 cm^3 HPGe detector made by ORTEC Company, USA, was 1.85 keV (FWHM) for the 1.33 MeV γ-ray of ^{60}Co. The γ-rays spectra were collected successively over a period varying from several hours up to two months to encompass the wide range of half-life of fission products involved, and to eliminate the cross interfering of the γ-ray from product nuclides of almost the same energy that can not be resolved by the HPGe detector.

Table 1 Fission product γ decay data used in fission yield measurement [11]

Product Nuclide	Energy (keV)	Half-life (min)	γ Intensity (%)
^{84g}Br	881.2	31.8	42
^{85m}Kr	304.9	268.8	14.0
^{87}Kr	402.6	76.3	49.6
^{88}Kr	196.3	170.4	25.58
^{89}Rb	1248.1	15.15	42.57
^{91}Sr	555.6	577.8	61.5
^{92}Sr	1384.1	162.6	90
^{93}Y	266.9	610.8	7.3
^{94}Y	918.8	18.7	56
^{95}Zr	756.7	92189	54.46
^{97}Zr	742.7	1014	93.06
^{99}Mo	739.5	3956.7	12.14
^{101}Tc	306.5	14.2	88
^{103}Ru	497.1	56526	90.9
^{104}Tc	358	18.3	89
^{105}Ru	724.2	266.4	47.3
^{112}Ag	617.5	187.8	43.5
^{115}Cd	336.3	3208.3	50.1
^{127}Sb	473.2	5544	25.6
^{128}Sn	482	59.1	59
^{131}I	637	11577.6	7.17
^{132}Te	228.3	4694.4	88.2
^{133}I	529.8	1248	87
^{134}I	847.1	52.6	95.4
^{135}I	1131.5	394.2	22.74
^{138}Cs	1435.8	33.41	76.3
^{140}Ba	537.3	18354	24.39
^{141}Ba	190.3	18.27	46
^{142}La	641.3	91.1	47.4
^{143}Ce	293.3	1980	42.8
^{146}Pr	453.9	24.15	48
^{147}Nd	531	15811.2	13.1

Table 2 Chain yields of ^{238}U fission induced by 22.0 MeV neutrons

Mass Number	Yield / %	error
84	0.79	±0.108
85	1.63	±0.096
87	1.90	±0.041
88	2.67	±0.052
89	3.68	±0.107
91	3.58	±0.019
92	3.94	±0.017
93	4.21	±0.237
94	3.99	±0.058
95	5.81	±0.089
97	6.09	±0.180
99	5.99	±0.103
101	5.03	±0.083
103	4.02	±0.024
104	3.67	±0.093
105	3.32	±0.025
112	1.63	±0.016
115	1.41	±0.040
127	1.78	±0.024
128	2.06	±0.865
131	3.96	±0.073
132	4.31	±0.053
133	5.69	±0.021
134	6.04	±0.178
135	6.03	±0.232
138	4.76	±0.126
140	4.05	±0.044
141	3.81	±0.213
142	3.52	±0.070
143	3.64	±0.019
146	2.18	±0.129
147	1.75	±0.140

2 Results and Discussion

The decay data used[11] and 32 chain yields measured are given in Table 1 and Table 2 respectively. The yields were calculated from the directly collected γ-ray spectra. For chain A→B→C, if half life of nuclides before A is much shorter than A's, B can be measured by gamma spectrum method, then accumulative yield of A can be calculated from:

$$Y_{\mathrm{A}}=\frac{AR_{\mathrm{B}}}{I_{\gamma}\varepsilon_{\gamma}Mf_{\mathrm{s}}f_{\Omega}f_{\mathrm{c}}f_{\mathrm{n}}\{\frac{\lambda_{\mathrm{B}}}{\lambda_{\mathrm{A}}(\lambda_{\mathrm{B}}-\lambda_{\mathrm{A}})}K_{\mathrm{A}}M_{\mathrm{A}}+(\frac{Y_{\mathrm{B}}}{\lambda_{\mathrm{B}}Y_{\mathrm{A}}}-\frac{\lambda_{\mathrm{A}}}{\lambda_{\mathrm{B}}(\lambda_{\mathrm{B}}-\lambda_{\mathrm{A}})})K_{\mathrm{B}}M_{\mathrm{B}}\}}$$

where $K_{\mathrm{A}}=[1-\exp(-\lambda_{\mathrm{A}}\Delta t)]\exp(-\lambda_{\mathrm{A}}\Delta t_1)$;

$K_{\mathrm{B}}=[1-\exp(-\lambda_{\mathrm{B}}\Delta t)]\exp(-\lambda_{\mathrm{B}}\Delta t_1)$;

$$M_{\mathrm{A}}=\sum_{i=1}^{n}N_i[1-\exp(-\lambda_{\mathrm{A}}\Delta T_i)]\exp(-\lambda_{\mathrm{A}}\Delta\tau_i);$$

$$M_{\mathrm{B}}=\sum_{i=1}^{n}N_i[1-\exp(-\lambda_{\mathrm{B}}\Delta T_i)]\exp(-\lambda_{\mathrm{B}}\Delta\tau_i);$$

AR_{B} is the peak area of gamma ray from decay of B; I_γ is the intensity; ε_γ is the detector efficiency for this γ-ray; M is mass of sample; N_i is fission rate monitored by double-fission chamber; f_s, f_Ω, f_c, and f_n are the correction factors of γ self-absorption, γ geometry, γ cascade coincidence losses and fission induced by background neutrons. After correction of independent yields on the decay chain after nuclide A, chain yields were got. Uncertainties (1σ) of the yields were obtained by consideration of all known sources of systematic and random errors such as mass determination of standard sample, detector efficiency of HPGe spectra system, statistic error of γ-ray peak area, and corrections, with the usual rules of error propagation. Uncertainties of decay data are not included. The complete mass distribution plotted in Fig.1 was derived from the chain yields. The sum of the yields directly measured was 64.15% for the light mass group, and 57.48% for the heavy mass group. To compare our data with other data published in literatures, some product yields are also shown in Fig.1. It can be seen that the fission yields increase with increasing neutron energy for the products in the valley region.

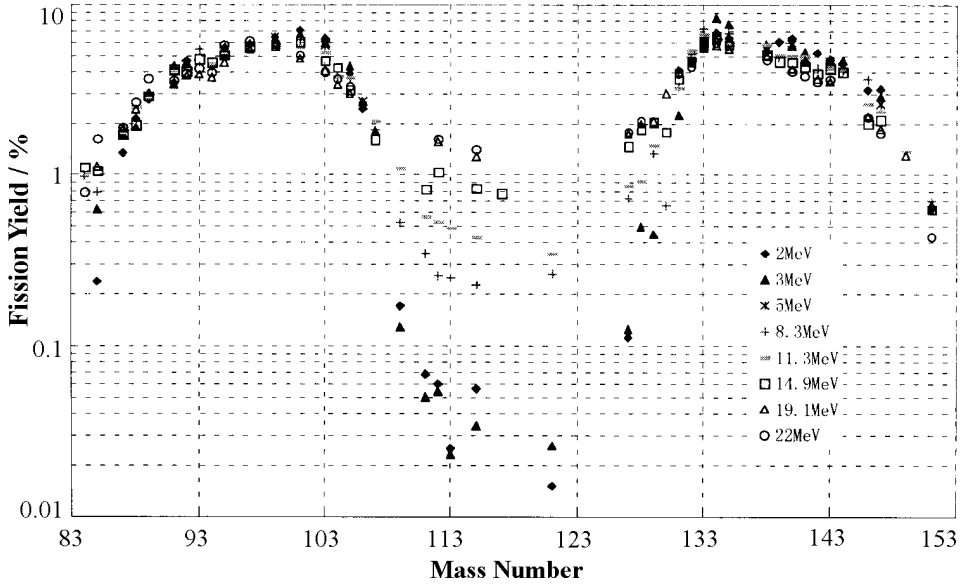

Fig. 1 Mass distribution of ^{238}U fission induced by neutrons

References

[1] LI Ze, et al., Precise determination of yields of ^{95}Zr, ^{140}Ba, and ^{147}Nd Chinese J. Nucl. Radiochem. 2, 1(1995)

[2] S. Nagy et al., Mass distribution in mono-energetic neutron induced fission of ^{238}U Phys, Rev. C 17, 163(1978)

[3] Champman, T, C. et al., Fission product yields from 6-9 MeV neutron -induced of ^{235}U and ^{238}U. Phys, ReV. C 17, 1089(1978)

[4] LI Ze et al., Mass distribution in 8.3 MeV neutron induced fission of ^{238}U. Chinese J. Nucl. Radiochem. 7, 97(1985)

[5] ZHANG Chunhua et al., Distribution of fission yields in the 3.0 MeV neutron induced fission of ^{238}U. Chinese J. Nucl. Radiochem. 7, 1(1985)

[6] WANG Xiuzhi et al., The absoluted determination of the cumulative yield of several nuclides from induced fission of ^{238}U by 5 MeV neutrons. Chinese J. Nucl. Radiochem. 6, 183(1984)

[7] SU Shuxin et al., The mass distribution in fission spectrum neutron induced fission of ^{238}U. Chinese J. Nucl. Radionchem. 13, 129(1991)

[8] LIU Chonggui et al., The mass distribution in 14.9 MeV neutron induced fission of ^{238}U. Chinese J. Nucl. Phys. 7, 235(1985)

[9] Nethaway et al., Low yield products from fission of ^{232}Th, ^{235}U, and ^{238}U with 14.8 MeV neutrons. Phys. Rev. 182, 1251(1969)

[10] QI Bujia et al., A tritium gas target for neutron production at HI-13 tandem accelerator. Atomic energy science and technology. 31, 385(1997)

[11] Richard B.Firestone.Table of Isotopes(EIGHTH EDITION),CDROM Edition, Version 1.0,March 1996

Measurement of Cross Section for ^{114}Cd (n, 2n) ^{113m}Cd Reaction at 14 MeV

ZHU Xuebin[1] ZHANG Feng[1, 2] KONG Xiangzhong[1]

1. Department of Modern Physics, Lanzhou University, Lanzhou, 730001

2. School of Geosciences and Information, University of Petroleum, Dongyin

【**abstract**】*The cross section of ^{114}Cd(n,2n)^{113m}Cd reaction was measured relatively to ^{93}Nb(n,2n)^{92m}Nb reaction at neutron energy of 14.7±0.3MeV, using the activation technique. The activities were measured with high resolution HPGe detector. The error of the measured cross section is 9.4%.*

Introduction

The neutron activation cross sections of 14 MeV are important for fusion study. Cadmium is an important material in a fusion reactor, but up to now, there are no data about the cross section for ^{114}Cd(n,2n)^{113m}Cd reaction. In this work, the cross section for ^{114}Cd(n,2n)^{113m}Cd reaction was measured by using the activation method at neutron energy of 14.7 MeV, using the ^{93}Nb(n, 2n)^{92m}Nb reaction as a standard.

1 Measurement

The irradiation of sample was carried out at the ZF-300-Ⅱ Intense Neutron Generator of Lanzhou University with the neutron yield about $(1\sim3)\times10^{12}$ s^{-1}. Neutrons were produced by T(d, n)^{4}He reaction with an effective deuteron beam energy of 125 keV and a beam current of 20 mA. The thickness of T-Ti target is 0.9 mg/cm^2. The neutron fluence was monitored with a uranium fission chamber so that the corrections could be made for variation of neutron yields during the irradiation. The samples were placed at the angle 0^o relative to the beam direction and were irradiated for 17.97 h. The cross section of the reaction was determined relatively to the cross section of ^{93}Nb(n, 2n) ^{92m}Nb reaction. The samples were made of natural metal foils. The cadmium sample was 30 mm in diameter, 0.8 mm in thickness and 99.99% in chemical purity. The niobium sample was 30 mm in diameter, 0.9 mm in thickness and 99.9% in purity. The cadmium sample was sandwiched between two niobium foils. The neutron energy was 14.7±0.3 MeV determined by the method of cross section ratio of zirconium and niobium[1].

After irradiation, the cadmium sample was cooled for 10.89 a. The activities of ^{113m}Cd and ^{92m}Nb were measured by using a CH8403 coaxial high purity germanium detector with a relative efficiency of 20% and an energy resolution of 3 keV at 1.33 MeV. The efficiency of the detector was calibrated using the standard gamma source (SRM4275) from the National Institute of Standard and Technology, USA[2]. The error of the absolute efficiency was estimated to be 2%. The decay data used in this study are taken from Ref. [3] and listed in Table 1.

Table 1 Decay data of products

α/%	Reaction	$T_{1/2}$	E_γ/ keV	I_γ / %
28.73	^{114}Cd(n, 2n) ^{113m}Cd	14.1 a	263.7	0.023
100	^{93}Nb(n, 2n) ^{92m}Nb	10.15 d	934.5	99.2

α: Abundance of target isotope

In the measurement of gamma-ray activities, some corrections were made for the effects of neutron intensity fluctuation, gamma-ray self-absorption in the samples, the sum peak effects in the investigated nuclide and the counting geometry, etc.

2 Results

The cross section was calculated by the following formula:

$$\sigma_x = \frac{[S\varepsilon I_\gamma \eta KMD]_o[\lambda AFC]_x}{[S\varepsilon I_\gamma \eta KMD]_x[\lambda AFC]_o}\sigma_o$$

Where σ_x, σ_o are the measured and standard cross-

sections, respectively; ε is full energy peak efficiency of the measured characteristic gamma ray; I_γ is gamma-ray intensity; η is abundance of the target nuclide; M is mass of sample; $D = e^{-\lambda t_1} + e^{-\lambda t_2}$ is counting correction factor (where t_1, t_2 are time intervals from the end of the irradiation to the start and finish of counting, respectively); A is atomic weight; C is measured full-energy peak area; $F=f_s f_c f_g$ is total correction factor of the activity (where f_s, f_c and f_g are the correction factors for the self-absorption in the sample for a given gamma energy and the sum effect of cascade gamma rays in the investigated nuclide as well as the counting geometry, respectively); and K is neutron fluctuation factor.

$$K = \sum_{i=1}^{L} [\Phi_i (1 - e^{-\lambda \Delta t_i}) e^{-\lambda T_i}] / (\Phi s)$$

Where L is number of time intervals, into which the irradiation time is divided; Δt_i is duration of the ith irradiation time; λ is decay constant; T_i is time interval from the end of the Δt_i to the end of irradiation; Φ_i is neutron fluence averaged over the sample in Δt_i; Φ is neutron fluence averaged over the sample in the total irradiation time T, S is factor $1-e^{-\lambda T}$.

The measured cross section for the ^{114}Cd(n, 2n) ^{113m}Cd reaction in this work is shown in Table 2.

Table 2 The measured cross sections

Reaction	E_n / MeV	σ / mb
^{114}Cd(n, 2n) ^{113m}Cd	14.7±0.3	432±41
^{93}Nb(n, 2n) ^{92m}Nb	14.7±0.3	458.2±9.2

The errors reported in this work are from counting statistics, standard cross section, detector efficiency, neutron energy, weight of samples, self-absorption of gamma ray, etc.

Reference

[1] QIU Jiuzi et al., Journal of Lanzhou University (Natu Sci), 1995, 31(4): 118

[2] WANG Yongchang et al., High Energy Phys & Nucl Phys. 1990, 14(10): 923

[3] R.B Firestone, Table of Isotopes, 8th edition, 1996

Measurement of Thermal Neutron Capture Cross Section

HUANG Xiaolong HAN Xiaogang YU Weixiang LU Hanlin ZHAO Wenrong

China Institute of Atomic Energy, P.O.Box 275(41) Beijing,102413

e-mail huangxl@iris.ciae.ac.cn

【abstract】 *The thermal neutron capture cross sections of $^{71}Ga(n,\gamma)^{72}Ga$, $^{94}Zr(n,\gamma)^{95}Zr$ and $^{191}Ir(n,\gamma)^{192}Ir^{m1+g,m2}$ reactions were measured by using activation method and compared with other measured data. Meanwhile the half-life of ^{72}Ga was also measured. The samples were irradiated with the neutron in the thermal column of heavy water reactor of China Institute of Atomic Energy. The activities of the reaction products were measured by well-calibrated Ge(Li) detector.*

Introduction

The thermal neutron capture cross sections of ^{71}Ga(n,γ)^{72}Ga, ^{94}Zr(n,γ)^{95}Zr and ^{191}Ir(n,γ)^{192}Ir$^{m1+g,m2}$ reactions are very important for evaluating the radiation damage of the material, especially for the metal Ir. The very accurate capture cross section is needed for Ir metal due to its larger capture cross section and longer half-life($T_{1/2}$=241 a). All measurements of other laboratories were performed before 1978, and there are large discrepancies among them. So new measurements are needed.

In present work, we measured the thermal neutron capture cross sections of $^{71}Ga(n,\gamma)^{72}Ga$, $^{94}Zr(n,\gamma)^{95}Zr$ and $^{191}Ir(n,\gamma)^{192}Ir^{m1+g,m2}$ reactions. The activation method was used and $^{197}Au(n,\gamma)^{198}Au$ reaction was taken as reference reaction.

1 Experiment Procedures

The experiments were performed in the thermal column of heavy water reactor of China Institute of Atomic Energy. The $^{197}Au(n,\gamma)^{198}Au$ reaction was taken as reaction to determine the absolute neutron fluence. The samples of $^{191}Ir(n,\gamma)^{192}Ir^{m2}$ reaction were irradiated in 1992 and its cooling time is 5a. The other measurements were performed in December 1997. Natural metal Ir and Zr plates were machined into the samples with 20 mm in diameter. The ^{71}Ga samples made of Ga_2O_3 powder were pressed into disks of 20 mm in diameter, 1 mm in thickness. The weight correction of Ga_2O_3 powder were made due to its little water-absorption in air.

After irradiation, the activities of the residual nuclei were measured with well-calibrated Ge(Li) detector. The decay data of the residual nuclei were taken from the reference [1] and listed in Table 1.

Table 1 Decay data of reaction products and standard cross-section

Reactions	$T_{1/2}$	E_γ/keV	I_γ/%	Standard cross section / b
$^{71}Ga(n,\gamma)^{72}Ga$	13.95 h	834.0	95.63±0.07	
$^{94}Zr(n,\gamma)^{95}Zr$	64.02 d	724.2	44.17±0.13	
$^{191}Ir(n,\gamma)^{192}Ir^{m1+g,}$	73.831 d	468.1 316.5	47.83±0.17 82.81±0.21	
$^{191}Ir(n,\gamma)^{192}Ir^{m2}$	241 a	316.5	82.81±0.21	
$^{197}Au(n,\gamma)^{198}Au$	2.6498 d	411.8	95.57±0.48	98.65±0.09

2 Results and Discussion

(1) The samples made of Ga_2O_3 powder were irradiated for 4 times. After the corrections of the weight and self-absorption in the ^{71}Ga sample, the final result is the average of the four measurements and listed in Table 2, with the other data taken from the reference BNL-325, (1971 and 1984). Present measurements are in agreement with recommended data by BNL-325 in the error bar.

Table 2 The cross-section of $^{71}Ga(n,\gamma)^{72}Ga$ reaction

Time	Author	Cross section / b
1947	L.Seren	3.36±0.67
1952	H.Pomerance	4.9±0.4
1959	Y.Starisski	4.0±0.7
1960	W.S.Lyon	6.18±0.62
1971	T.B.Ryres	4.71±0.27
1975	G.Gleason	4.40±0.20
1978	R.E.Heft	4.74±0.10
1984	L.Koester	3.69±0.10
1981	BNL-325	4.71±0.23
1998	Present work	4.62±0.09

In present work, the half-life of ^{72}Ga was also measured. The measurements were performed in 2 times. By means of the non-linear least squares method, the final result of the half-life of ^{72}Ga is:

$$T_{1/2}=13.95\pm0.05 \text{ h}.$$

(2) Present measurements and other data for $^{191}Ir(n,\gamma)^{192}Ir^{m1+g,m2}$ reactions are listed in Table 3.

Table 3 The cross-section of $^{191}Ir(n,\gamma)^{192}Ir^{m1+g,m2}$ reactions

Time	Author	m_1+g (b)	m_2 (b)
1947	L.Seren	1000±200	
1963	B.Keish	910±90	
1963	G.Harbottl		0.38±0.24
1964	H.Arinu	1200±300	
1968	B.Sims	1120±25 1166±26	
1978	R.E.Heft	922±13	
1984	BNL-325	954±10	0.16±0.07
1998	Present work	855±13	0.14±0.06

There is only one datum for $^{191}Ir(n,\gamma)^{192}Ir^{m2}$ reaction measured by G.Harbottle in 1963 before present work. In his experiment, the cross section of $^{191}Ir(n,\gamma)^{192}Ir^{m1+g}Ir$ was used as the reference cross section to determine the neuron fluence, and the half-life was 600 a. If 954 b (evaluated by BNL-325) as reference cross section and 241 a as half-life are used

the datum 0.38±0.24 b would be changed becomes to 0.15±0.07 b, which is consistent with present measurement.

Present measurement of the cross section for the m_1+g state is about 10% lower than the data measured by other laboratories (BNL-325, 1971 and 1984).

(3) Present measurements and other data(BNL-325, 1971 and 1984) for $^{94}Zr(n,\gamma)^{95}Zr$ reaction are listed in Table 4. The present result is in agreement with the data of BNL-325 in the range of measured errors.

Reference

[1] Richard B.Firestone,Virginia S.Shirley. Table of Isotopes eighth Edition, March 1996

Table 4 The cross-section of $^{94}Zr(n,\gamma)^{95}Zr$ reaction

Time	Author	Cross section / b
1952	H.Pomerance	0.08±0.04
1955	W.A.Brooksbank	0.06±0.01
1960	W.S.Lyon	0.075
1970	M.D.Ricabarra	0.063±0.008
1971	R.H.Fulmer	0.052±0.003
1973	D.C.Santry	0.0475±0.0024
1978	R.Kundberg	0.052
1978	R.E.Heft	0.055±0.002
1982	J.M.Wyrick	0.0494±0.0017
1971	BNL-325	0.056±0.004
1981	BNL-325	0.0499±0.0024
1998	Present work	0.053±0.002

Chain Yields from 19.1 MeV Neutron-induced Fission of ^{235}U

BAO Jie YANG Yi LIU Yonghui FENG Jing LI Ze CUIui Anzhi SUN Hongqing
ZHANG Shengdong GUO Jingru
CIAE,P.O.BOX 275-46,Beijing 102413,PRC
e-mail jie-bao-99@163.net.

【**abstract**】*Chain yields for 35 mass chains were determined for the fission of ^{235}U induced by 19.1MeV neutrons for the first time. Absolute fission rate was monitored with a double fission chamber; fission product activities were measured by HPGe γ-ray spectrometry. Threshold detector method was used to measured the neutron spectrum in order to estimate the fission events induced by break-up neutrons and scattering neutrons from the environment. A mass distribution curve has been obtained.*

Introduction

The fission product mass distribution of ^{235}U has been extensively investigated, for some fission induced by monoenergic neutrons, but no more than 19 MeV neutron [1],[2]. In the present work, the chain yield of ^{235}U fission induced by 19.1 MeV neutrons was measured by means of γ-ray spectrometry.

1 Experiment

The experiment was carried out at the 2×1.7 MeV Tandem ,CIAE. The 19.1 MeV neutron was produced by $T(d,n)^4He$ reaction. The Tritium-Ti target, which was used to produce neutrons by the bombardment with the deuteron beam, was of the size Φ10 mm and 5.2 mg/cm^2 in thickness. The deuteron beam energy was 3 MeV. The neutron spectrum was measured by threshold detector method in order to estimate the fission events induced by the background neutrons from the $T(d,np)^3H$ reaction and from the scattering by the environment. The ratio of background neutron fission events to 19.1 MeV neutron fission events was estimated to be 0.574:1.

The sample used in the irradiation were Φ16 mm disks of uranium metal of about 2 g, the abundance of Uranium isotopes is 90.2% for ^{235}U, 1.1% for ^{234}U, 0.3% for ^{236}U and 8.4% for ^{238}U. The uranium disks were sealed in a pure Al foil of 0.2 mm thickness. The sample, which was sandwiched between two standardized thin samples to monitor the fission rate absolutely[3], was mounted in a double fission chamber. The standardized thin samples were made of the same uranium as the thick ones. The double

fission chamber was covered with Cd of 1 mm thick in order to shield it from the thermal neutrons from the environment. 4 samples were irradiated for a period about 30 hours at a distance of about 5 cm from the neutron source in the direction of zero degree.

After the irradiation of γ-ray activities, the samples were measured by HPGe γ-spectrometers in turns. The γ-ray spectra were collected successively over a period varying from 30 seconds up to two months to encompass the wide range of half-lives of fission products involved, and to eliminate the cross interfering of the γ-ray from the product nuclides of almost the same energy which can not be resolved by the HPGe detector. And then, the γ-ray spectra were analyzed by the decay program SPAN[4]. The fission yields were obtained by program FYAUTOLS.

Table 1 Chain yields from 19.1MeV neutron-induced fission of ^{235}U

mass number	Yields / %	error
84	0.61	±0.16
85	1.49	±0.07
87	2.76	±0.04
88	3.21	±0.04
89	3.90	±0.05
91	3.87	±0.04
92	4.49	±0.09
93	4.22	±0.07
94	4.19	±0.05
95	4.54	±0.04
97	4.77	±0.03
99	5.6	±0.03
101	3.83	±0.04
103	3.06	±0.03
104	3.33	±0.06
105	2.92	±0.06
112	2.31	±0.11
115	2.02	±0.06
117	1.65	±0.11
127	2.29	±0.07
128	2.55	±0.64
129	2.79	±0.09
131	4.04	±0.54
132	3.82	±0.03
133	5.21	±0.03
134	6.25	±0.47
135	5.44	±0.04
138	4.38	±0.12
140	3.93	±0.04
142	2.97	±0.05
143	3.17	±0.05
146	1.54	±0.12
147	1.71	±0.07
149	0.85	±0.05
151	0.64	±0.05

2 Results and Discussion

The chain yields of 35 product mass chains were obtained. They are presented in table1. The fission product γ decay data used in these measurements were taken from *The Table of Isotopes (8th)*[5]. Corrections were made for coincidence losses, pile-up losses in the counting system, influence of the background neutrons, self absorption of γ-ray, independent yields, and influnence from other uranium isotope. The chain yields measured was plotted in Fig. 1. The sum of the yields directly measured was 61.1% for the light mass group, and 53.2% for the heavy mass group. Including the mass yields not measured but obtained by interpolating or extraporlating, the sum was 100.4% for the light mass group and 98.8% for the heavy mass group. Both of them are in good agreement with 200%. This demonstrates that we monitored the absolute fission rate and detected fission products to a very good precision. The mean mass numbers are 97.9u and 133.8u for the light and heavy mass group respectively, which give the mean fission neutron number $\hat{\nu}$=4.3. To compare our data with other data published in literatures, some product yields published by other authors[6,7] are also shown in Fig. 1. They display the dependence of fission yield with neutron energy.

3 Acknowledgement

The authors are indebted to professor LU Hanlin and Mr WANG Yihua.

References

[1] Glendenin LE, Gindler JE, Henderson DJ, et al. Mass sion Qistributions for Monoenergetic-Neutron-Induced Fission of ^{235}U. Phys Rev, C24,2600(1981)

[2] Chapman TC, Angelon CA, Spitals CC, et al. Fission Product Yields From 6-9MeV Neutron-Induced Fission of ^{235}U and ^{238}U. Phys Rev, C17,1089(1978)

[3] 李泽，王连壁，王维国等. 裂变率的绝对测量，原子能科学技术，5,600(1980)

[4] Wang Liyu. Multiplet Processing in High Resolution Gamma Spectroscopy. Appl Radiat Isot, 40,575(1989)

[5] Richard B.Firestone.Table of Isotopes(EIGHTH EDITION),CDROM Edition, Version 1.0,March 1996

[6] The absoluted determination of the cumulative yield of several nuclides from induced fission of ^{235}U by 14.9 MeV neutrons. Chinese, J, Nucl, Radio chem, Vol, 6, No.3,183(1984)

[7] James MF,Mills RW,Weaver DR.A New Evaluation of Fission Product Yields and the Production of a New Library(UKFYZ) of Independent and Cumulative Yields.Part II.Tables of Measured and Recommended Fission Yields:AEA-TRS-1018.1991

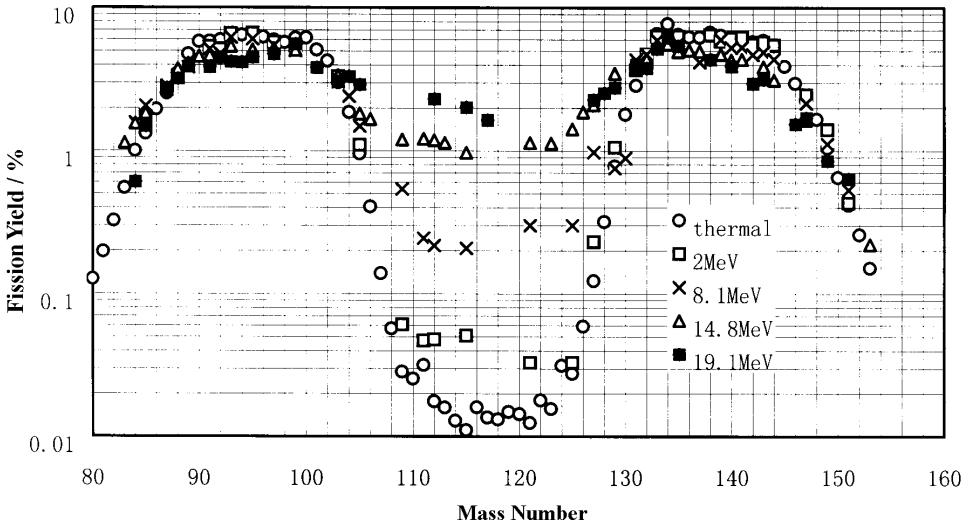

Fig. 1 Chain yields from monoenergetic-neutron-induced fission of ^{235}U

Evaluation of Complete Neutron Nuclear Data for $^{204, 207}Pb$

MA Gonggui

Institute of Nuclear Science and Technology, Sichuan University, Chengdu, 610064

【**abstract**】*The complete neutron data were evaluated in the energy range from 10^{-5} eV to 20.0 MeV for ^{204}Pb and ^{207}Pb. The data include total, elastic, nonelastic, total inelastic, inelastic to 11 and 16 discrete levels, inelastic to continuum states, (n,2n), (n,3n), (n,n'p), (n,p), (n,t), (n,α) and capture cross sections. The angular distributions of secondary neutron, the double differential cross sections (DDCS), the gamma-ray production data and the resonance parameters are also included. The evaluated data were adopted into CENDL-3 in ENDF/B-6 format.*

Introduction

Lead is a very important structure material in nuclear fusion engineering. The complete neutron nuclear data were evaluated on the basis of both experimental data measured up to 1999 and theoretical calculated data with program UNF[1]. The evaluated data were adopted into CENDL-3 in ENDF/B-6 format.

For natural lead, the data of all reaction channels are in very good agreement with the sum of the all isotopes′ data weighted by the abundance in the error range.

The level scheme is given in Table 1, selected from new data of Ref. [2].

Table 1 Levels sheme of ^{204,207}Pb

^{204}Pb(1.4%)		^{207}Pb(22.1%)	
E_1 / MeV	J^π	E_1 / MeV	J^π
0.0	0^+	0.0	0.5^-
0.8992	2^+	0.5698	2.5^-
1.2739	4^+	0.8977	1.5^-
1.3514	2^+	1.6334	6.5^+
1.5631	4^+	2.3400	3.5^-
1.5836	0^+	2.6232	2.5^+
1.6047	3^+	2.6624	3.5^+
1.6650	2^+	2.7030	3.5^+
1.6820	1^+	2.7280	4.5^+
1.7300	0^+	3.2230	5.5^+
1.7619	1^-	3.3000	0.5^+
1.8173	4^+	3.3840	4.5^+
		3.4130	4.5^-
		3.5090	5.5^+
		3.5830	4.5^+
		3.620 0	4.5^+
		3.6340	2.5^+

1 Resonance Parameter

The resolved resonance parameters, taken from ENDF/B-6, were given from 10^{-5} eV to 0.05 MeV for ^{204}Pb and 0.475 MeV for ^{207}Pb; thermal cross sections of (n,tot), (n,n) and (n,γ) reactions are 11.857 b, 11.197 b and 0.661 b for ^{204}Pb; 11.459 b, 10.747 b and 0.712 b for ^{207}Pb, respectively.

2 Neutron Cross Section

The comparison of experimental data with evaluated ones is shown in Fig.1~10. It can be seen that the present evaluation is in agreement with the experimental data.

2.1 Total Cross Section

Above the resolved resonance region, there is still a small structure energy range (0.475~5.0 MeV) and then smooth energy range (5.0~20.0 MeV). For ^{207}Pb in the energy range from 0.475 to 20.0 MeV, the data were mainly taken from ENDF/B-6 data; the corresponding experimental data of Koehler, Horen, Benetskij, Dukarevich and Day[3-7] for ^{207}Pb are given in Fig. 1. For ^{204}Pb in the energy range from 0.05 to 20.0 MeV, the data were mainly taken from JENDL-3.1 data; the corresponding experimental datum of Dukarevich for ^{204}Pb is given in Fig. 2.

2.2 Elastic Scattering Cross Section

The elastic scattering cross section was obtained by subtracting the sum of cross sections of all the non-elastic processes from the total cross section. In general, the agreement between the evaluated cross section and the available experimental data of Guenther, Tomita and Day[9~11] is good for ^{207}Pb.

2.3 Nonelastic Scattering Cross Section

This cross section is the sum of all cross sections of nonelastic channels (n,n′), (n,2n), (n,3n), (n,n′p), (n,γ), (n,p), (n,t) and (n,α) reactions.

2.4 Total Inelastic Cross Section

The total inelastic cross sections were taken from the calculations (see Fig. 3~4).

2.5 Inelastic Cross Section to the Discrete Levels and the Continuum

The inelastic scattering cross section to 16 discrete levels were calculated by using UNF code. For 0.5697, 0.8977, 1.6334 and 2.34 MeV levels of ^{207}Pb, the experimental data measured by Almen-Ra., Cranberg and Kinney[12~14], were used to normalize the corresponding model calculated results. The plots of these data and the evaluated data are shown in Figs. 3-1, 3-2. For other levels, the data were taken from calculated results. The inelastic scattering cross section to 11 discrete levels of ^{204}Pb were calculated by using UNF code.

The continuum part was obtained by subtracting the cross section of inelastic scatteringe to discrete levels from the total inelastic cross section.

2.6 (n,2n) and (n,3n) Cross Section

For (n,2n) reaction of ^{207}Pb, the experimental data were measured by Frehaut[15] in the energy range from 7.41 to 14.76 MeV, The evaluated data were obtained by spline function fitting experimental data. Above 14.76 MeV, calculated data were nomalized to fitting value of the experimental data at 14.0 MeV (see Fig. 5).

For (n,2n) reaction of ^{204}Pb, the experimental data were measured by Filatenkov, Lu Hanlin, Ikeda, Kobayashi, Ryves, Decowaki, Maslov, Drushinin, Dilg and Vaughn[16~25] in the energy range from 10.1 to 19.2 MeV. The evaluated data were obtained by spline function fitting experimental data (see Fig. 6).

The (n,3n) cross section was taken from the model calculation due to lack of the experimental data.

2.7 (n,p), (n,n'p), (n,α), (n,γ) Cross Sections

The cross sections were all taken from the model calculations (Fig. 7 for ^{207}Pb (n,γ) reaction).

2.8 (n, t) Cross Section

For ^{204}Pb (n,t) cross section, the calculated data were normalized to fit value of the experimental data of Qaim and Woo[26,27] at 14.6 MeV (see Fig. 8).

The ^{207}Pb (n,t) cross section was taken from the model calculation.

3 Secondary Neutron Angular Distributions

For elastic scattering angular distribution, the experimental data measured by Guenther, Tomita and Day were used to adjust the optical model parameters in the calculations. The calculated results in good agreement with the experimental data for ^{207}Pb (see Figs. 9~10).

The discrete level inelastic angular distributions were obtained from theoretical calculation results for both ^{207}Pb(MT=51~86) and ^{204}Pb (MT=51~11).

4 The Double Differential Cross Section and γ-Ray Production Data

The double differential cross section (MF=6, MT = 16, 17, 22, 28, 91, 103, 105, 107) and γ-ray production data (MF=12,13,14,15) were all taken from the calculation results for both ^{207}Pb and ^{204}Pb.

5 Theoretical Calculation

An automatically adjusted optical potential code (APOM)[28] was used for searching a set of optimum neutron spherical optical potential parameters. DWUCK code was used to calculate the direct inelastic scattering for excited levels taken as the input data of UNF. UNF code, including optical model, Hauser-Feshbach statistical model and exciton model, was used to calculate the data of files 3, 4, 6, 12, 13, 14, 15. The input parameters are optical potential, level density, giant dipole resonance[29] and nuclear level scheme. These patameters were adjusted on the basis of experimental data in the neutron energy range from 1 keV to 20 MeV.

5.1 Optical Model, Level Density and Giant Dipole Resonance Parameters

Optical potential parameters used are given in Table 2. The level density and pair correction parameters are given in Table 3, 4. The giant dipole resonance parameters are shown in Table 4. The symbols CSG, EE and GG in Table 5 are the peak cross section, resonance energy and full width at half maximum, respectively.

5.2 The Coupled Channel Calculation

The legendre Coefficients (L. C) of direct elastic scattering to ground state and direct inelastic scattering to excited states were calculated with coupled channel code DWUCK at 12 energies by Shen Qingbiao in the required input format of UNF.

Table 2 Neutron optical model potential parameters*

Depth / MeV		Radius / fm	Diffuseness / fm
V_0=46.945	W_0=3.805	X_r=1.24715	A_r=0.64
V_1=-0.232	W_1=0.4151	X_s=1.24	A_s=0.48
V_2=-0.00	W_2= 0.00	X_v=1.24	A_v=0.48
V_3=0.00	U_0=-0.0	X_{so}=1.24715	A_{so}=0.64
V_4=0.0	U_1=0.0	X_c=1.22	
V_{so}=6.0	U_2=0.0		

*Note: $V_r(E)=V_0+V_1E+V_2E^2+V_3(A\text{-}2Z)/A+V_4Z/A(1/3)$;
$W_s(E)=W_0+W_1E+W_2(A\text{-}2Z)/A$;
$U_v(E)=U_0+U_1E+U_2E^2$.

Table 3 Level density parameters and Pair correction values of 11 excess nuclei*

		n,γ	n,n'	n,p	n,α	n,^{3}He	n,d
^{204}Pb	*L*	7.73	10.1	7.34	13.97	11.03	9.64
	P	0.85	1.32	0.25	0.83	1.25	0.72
^{207}Pb	*L*	3.62	4.57	3.24	7.28	5.622	4.18
	P	1.18	0.60	0.58	1.14	0.71	0.0

		n,t	n,2n	n,n'α	n,2p	n,3n	
^{204}Pb	*L*	12.6	13.02	12.9	8.75	11.94	
	P	0.3	0.9	1.69	0.78	1.76	
^{207}Pb	*L*	5.86	6.25	8.75	4.69	7.73	
	P	0.61	1.21	0.78	1.11	0.85	

*Note: $L=[0.00880(s(z)+s(n))+Q_b]A$; $P=p(n)+P(z)$;
Q_b=0.142 or 0.12 (spherical or deformation).

Table 4 The 11 giant dipole resonance parameters (single peak)

^{204}Pb	CSG / b	0.481,0.541,0.541,0.481,0.645,0.541, 0.645,0.541,0.645,0.645,0.645,
	EE / MeV	13.56,13.72,13.72,13.56,13.63,13.72, 13.63,13.72,13.63,13.63,13.63,
	GG / MeV	3.96,4.61,4.61,3.96,3.94,4.61,3.94, 4.61,3.94,3.94,3.94,
^{207}Pb	CSG / b	0.65,0.481,0.481,0.54,0.481,0.54, 0.481,0.481,0.645,0.54,0.481
	EE / MeV	13.63,13.6,13.6,13.72,13.6,13.72, 13.6,13.6,13.63,13.72,13.6
	GG / MeV	3.94,3.96,3.96,4.61,3.96,4.61,3.96, 3.96,3.94,4.61,3.96,

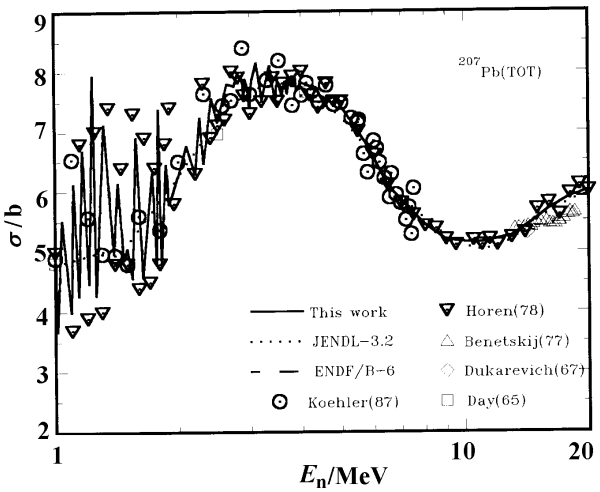

Fig. 1 Total cross section for ^{207}Pb

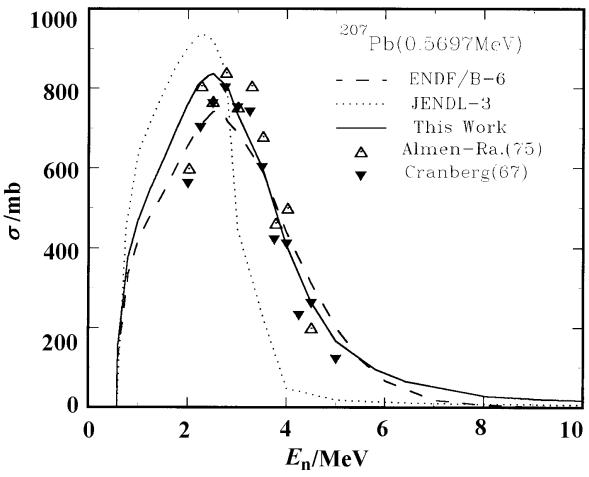

Fig. 3-1 Inelastic cross section for ^{207}Pb excited states

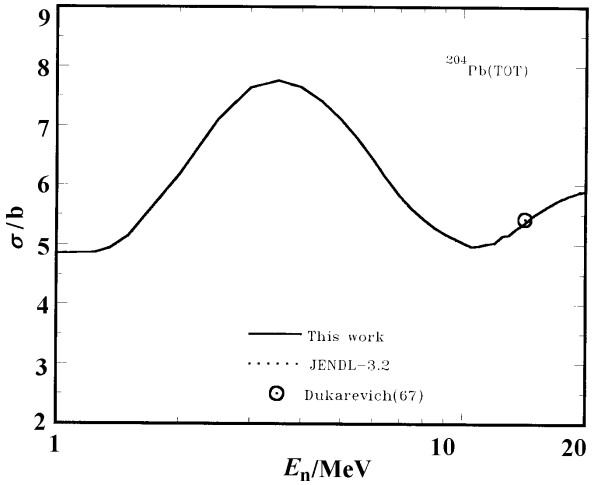

Fig. 2 Total cross section for ^{204}Pb

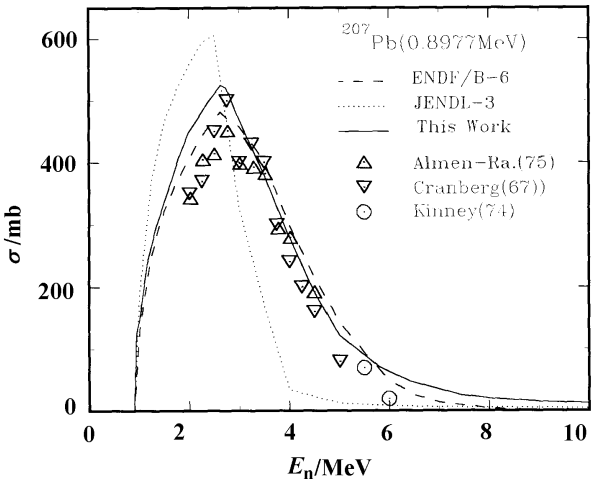

Fig. 3-2 Inelastic cross section for ^{207}Pb excited states

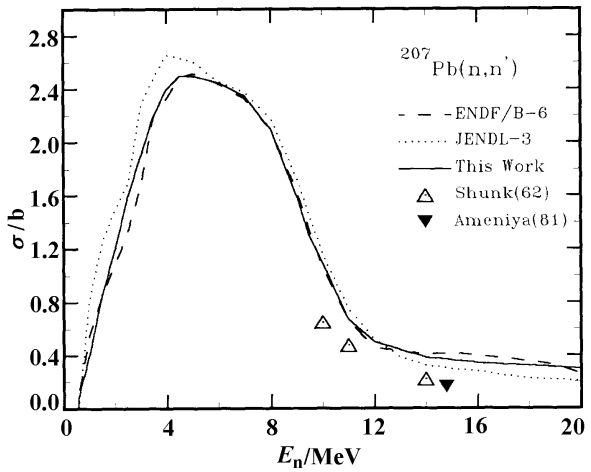

Fig. 3 Inelastic cross section for ^{207}Pb

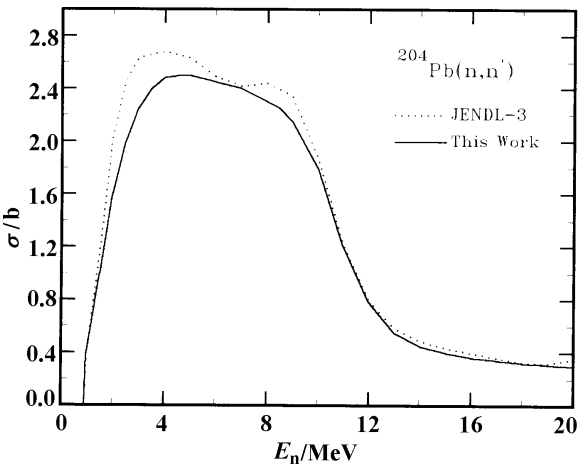

Fig. 4 Inelastic cross section for ^{204}Pb

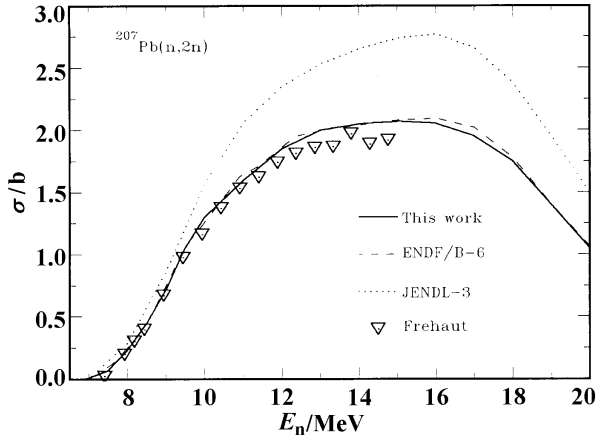

Fig. 5 (n,2n) cross section for ^{207}Pb

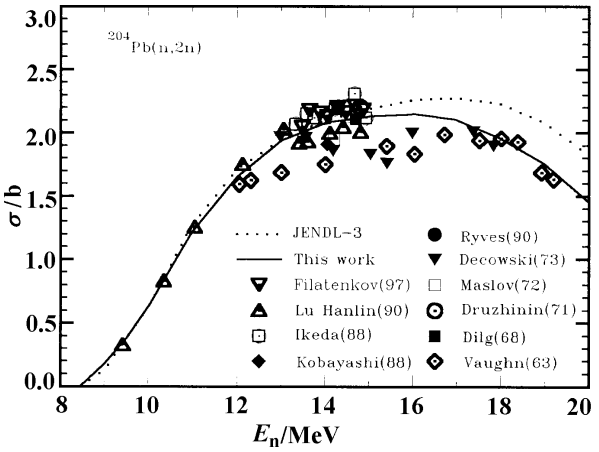

Fig. 6 (n,2n) cross section for ^{204}Pb

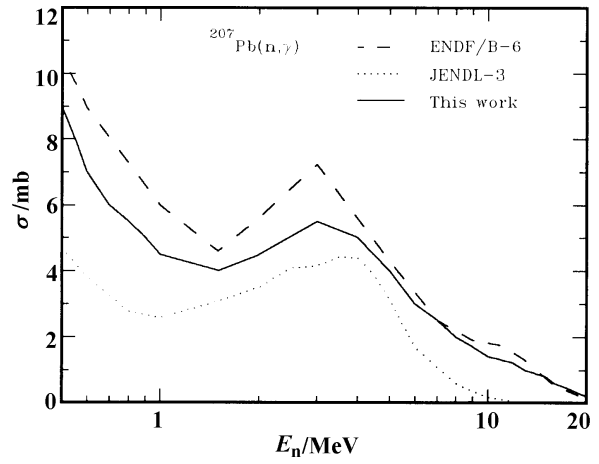

Fig. 7 (n,γ) cross section for ^{207}Pb

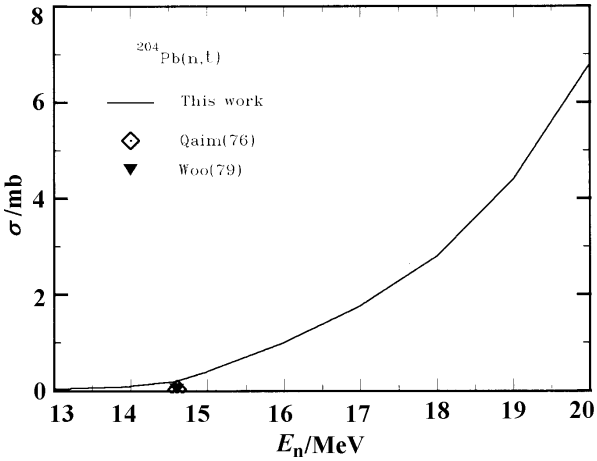

Fig. 8 (n,t) cross section for ^{204}Pb

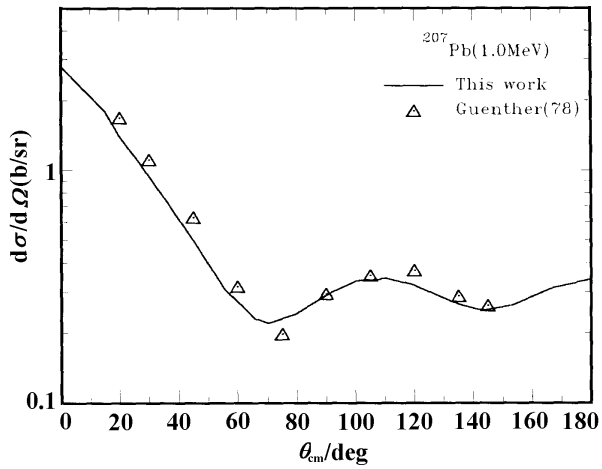

Fig. 9 Elastic scatter angular distribution of ^{207}Pb

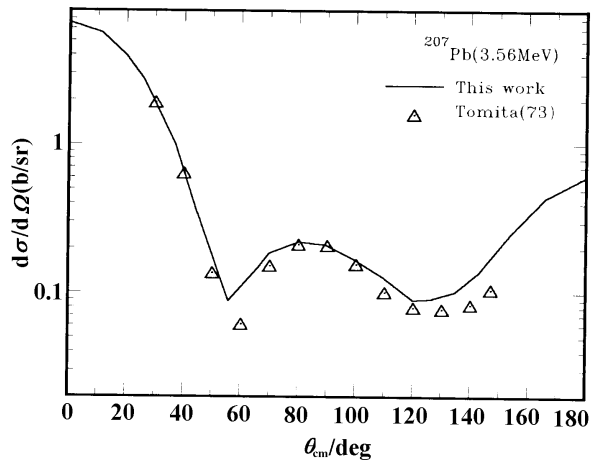

Fig. 10 Elastic scatter angular distribution of ^{207}Pb

6 Concluding Remarks

Due to the new experimental data have been available in last years, the evaluated data were considerably improved, especially for the cross sections of (n,2n) reaction and inelastic scattering to some discrete levels.

Acknowledgments

The author would like to thank Prof. LIU Tingjin for his much helps with this work, also thank Prof. Shen Qingbiao for his help in the DWUCK code calculation.

References

[1] ZHANG Jingshang. Nucl. Sci. Eng., 1993, 114; 55~63

[2] Nuclear Data Sheets, 43, 383, 1984; 61, 93, 1990; 47,797,1986; 63,723,1991; 50,719,1987

[3] R.Koehler et al. Phys. Rev., C35,1646(1987)

[4] D.J.Horen et al. Phys. Rev., C18,722(1978)

[5] B.A.Benetskij et al. 77Kiev 2,47(1977)

[6] Ju.V.Dukarevich et al. Nucl. Phys., A92(2),433(1967)

[7] R.B.Day et al. EXFOR 12191.1010(1965)

[8] D.J.Horen et al. Phys. Rev., C29,2126(1984)

[9] P.T.Guenther et al. Nucl. Sci. Eng., 65,174(1978)

[10] Y.Tomita et al. EXFOR 20304.002(1973)

[11] R.B.Day et al. EXFOR 12191.009(1965)

[12] E.Almen-Ra. et al. Atomnaya Energiya, 503(1975)

[13] L.Cranberg et al. Phys. Rev.,159,969(1967)

[14] W.E.Kinney et al. ORNL-4909(1974)

[15] J.Frehaut et al. BNL-NCS-51245(1980)

[16] A.A.Filatenkov et al. EXFOR 41240.069(1997)

[17] LU Hanlin et al. C. Nucl. Phys., 12,269(1990)

[18] Y.Ikeda et al. JAERI-1312(1988)

[19] K.Kobayashi et al. 88MITO,261(1988)

[20] T.B.Ryves et al. ANE 17,107(1990)

[21] P.Decowaki et al. Nucl. Phys., A204,121(1973)

[22] G.N.Maslov et al. EXFOR 40136.001(1972)

[23] A.A.Drushinin et al. EXFOR 40171(1971)

[24] W.Dilg at al. Nucl. Phys., A118,9(1968)

[25] F.J.Vaughn et al. EXFOR 12223.002(1963)

[26] S.M.Qaim EY AL. Nucl. Phys., A257(2),233(1976)

[27] T.W.Woo et al. 79KNOX, 853(1979)

[28] SHEN Qingbiao et al. CNDP, No.7, 43(1993)

[29] ZHUANG Youxiang et al. Chinese Physics, 8, 721-727(1988)

Evaluation of Nuclear Fission Barrier Parameters for 17 Nuclei

WANG Shunuan

China Nuclear Data Center, CIAE, P.O.Box 275(41) Beijing, 102413

e-mail wsn@iris.ciae.ac.cn

As we know well that modern nuclear installations and applications have reached a high degree of sophistication. The effective safe and economical design of these technologies require detailed and reliable design calculations. The accuracy of these calculations is largely determined by the accuracy of the basic nuclear and atomic input parameters. In order to meet the needs on high energy fission cross section, fission spectra in waste disposal, transmutation, radioactive beams physics and so on, 17 nuclei fission barrier parameters were collected from the literature based on different experiments and

measurements as well as some theory models, and evaluated. The 17 nuclei include some ultra neutron-deficient nuclei and some short half-life radioactive ones. These parameters can be used for nuclear model calculation of nuclear reaction cross sections, spectra and other related important physical quantities required by a large variety of applications.

In fission barrier parameters research for the ultra neutron-deficient nuclei[1], the reduced probabilities of the delayed fission channel $P_{\beta df}$ for $^{188}_{83}$Bi and $^{196}_{85}$At were determined from experimental data as 3.4×10^{-4} and 8.4×10^{-4}, respectively. The comparison of the obtained and calculated values of $P_{\beta df}$ allows one to estimate the fission barrier parameters for ^{188}Pb^{82} and ^{196}Po^{84} by using statistical model calculations. The results are as the following:

$^{188}_{82}$Pb $B_f = 9.6 \pm 0.9$ MeV

$^{196}_{84}$Po $B_f = 8.6 \pm 0.9$ MeV (case (1))

$B_f = 8.2 \pm 0.6$ MeV

$B_f = 7.4 \pm 0.6$ MeV (case(2))

with $\hbar\omega = 1$ MeV

Here, case (1) and case (2) are for two different assumptions about Γ_f/Γ_{tot} in statistical model calculations. Γ_f is the fission width and Γ_{tot} is total decay width. In case (1), $\Gamma_f = 0.5\Gamma_{tot}$ was used. In case (2), Γ_f was calculated by using an expression recommended in Ref. [2] in which the Hill-Wheeler formula was used and the radioactive capture decay width Γ_γ was calculated by using the formula presented by A.Stoliry et al.[3] . In the whole statistical model calculations, the Gilbert-Cameron level density formula was utilized.

The liquid-drop fission barrier B_f^{LD} is smaller than the full fission barrier by a value of the shell correction, which is equal to 1.2 MeV for $^{188}_{82}$Pb and 1.8 MeV for $^{196}_{84}$Po according to the calculations of Ref.[4]. The results of B_f^{LD} obtained from the experimental data on the delayed fission probability in Ref.[1] in case (2) and the corresponding shell correction calculation mentioned above, are in good agreement with fission barrier obtained from data on cross section of heavy ion reactions for these nuclei[5,6]. The values of B_f^{LD} obtained from the experimental data on the delayed fission data are also not in contradiction with the assumption about a more rapid decrease of the fission barrier for neutron-deficient nuclei than it is predicted by the theory. Besides, there should be some other factors that can influence the fission barrier height. These factors could be, for instance, the resonance structure of the β-decay strength function; the influence of spin states and the structure of energy levels as well as occupied at β-decays on the value of Γ_f; the contribution of delayed charged particle like proton and alpha decays to the value of Γ_{tot}. But all of these factors can cause only an additional decrease of the barriers. Therefore, based on the above analysis we recommend fission barrier parameters of Ref. [1] in case 2 for $^{188}_{82}$Pb and $^{196}_{84}$Po as the following:

$^{188}_{82}$Pb $B_f = 8.2 \pm 0.6$ MeV

$^{196}_{84}$Po $B_f = 7.4 \pm 0.6$ MeV (with $\hbar\omega = 1$ MeV)

M. Thoennessen and G. F. Bertsch presented the empirical domain of validity of statistical theory[7] , as applied to fission data on pre-fission neutron, charged particle and γ-ray multiplicity. Systematic analysis are found of the threshold excitation energy for the appearance of non-statistical fission. In this paper, they search for systematic trends of the validity of the statistical model by assembling data over a wide range of masses and fissilities. In particular, they tabulated the threshold excitation energy E_{thresh} marking the upper limit of the energies where the statistical theory applies; they extracted and analyzed the threshold excitation energy and the fission barrier from a variety of different measurements. They listed the analyzed fission system following fusion evaporation reactions. The pre-fission neutron, charged particle and GDR γ-ray multiplicity measurements are also included (See Table 1).

Table 1 Different Reactions, Compounds and their Paramenters

Reaction	CN	x_{fiss}	E_{thresh}	B_f	Ref.
^{16}O+^{142}Nd	^{158}Er	0.60	80±10	11.2±2.0	[8]
^{18}O+^{150}Sm	^{168}Yb	0.60	85±5	10.4±2.4	[9]
^{19}F+^{159}Tb	^{178}W	0.64	80±10	10.3±2.3	[10]
^{19}F+^{169}Tm	^{188}Pt	0.67	80±5	7.1±1.2	[10]
^{28}Si+^{170}Er	^{198}Pb	0.70	60±5	7.1±1.1	[9]
^{19}F+^{181}Ta	^{200}Pb	0.70	65±5	8.6±1.0	[9]
^{30}Si+^{170}Er	^{200}Pb	0.70	55±5	7.0±0.9	[9]
^{18}O+^{192}Os	^{210}Po	0.71	60±5	8.0±0.8	[9]
^{16}O+^{197}Au	^{213}Fr	0.74	45±5	6.2±0.6	[11]
^{16}O+^{208}Pb	^{224}Th	0.76	30±5	5.5±0.5	[12]
^{19}F+^{232}Th	^{251}Es	0.83	20±10	1.8±0.2	[10]
p+^{238}U	^{239}Np	0.78	20±2	4.3±0.1	[13]
^{28}Si+^{164}Er	^{192}Pb	0.72	58±5	5.9±0.9	[14]
^{28}Si+^{164}Er	^{192}Pb	0.72	53±5	6.7±0.9	[14]
^{19}F+^{181}Ta	^{200}Pb	0.70	68~84	8.4~6.5	[15]
^{32}S+^{184}W	^{216}Th	0.78	72~85	2.6~1.7	[16]
^{16}O+^{208}Pb	^{224}Th	0.76	30~40	5.5~4.5	[17]
^{32}S+^{208}Pb	^{240}Cf	0.84	67~80	0.7~0.4	[18]

CN: Compound Nuclei ; x_{fiss} :Fissilities; E_{thresh}:Threshold energies; B_f:Mean fission barrier; All energies are in MeV, the same below.

In present paper we are interested in compound nuclei (CN), fissilities(x_{fiss}), and mean fission barrier B_f listed in Table 1. We notice that there are two values taking from different measurements for ^{200}Pb and ^{192}Pb, respectively. In this case we recommend the mean value of them with weight and its external error. Thus we have B_f =7.8±0.67 MeV for ^{200}Pb and 6.3±0.64 MeV for ^{192}Pb. The result of B_f=7.8±0.67 MeV for ^{200}Pb is just in the range of 8.4~6.5 MeV taking from measurement[15] (also listed in Table 1). It is clear that the results from different works are in agreement with each other. From the listed results in table 1, it can be seen clearly also that the result of B_f =5.5±0.5 MeV for ^{224}Th taking from Ref. [12] is in agreement with the result of B_f=5.5~4.5MeV taking from Ref. [17].

Table 2 listed the results of peripheral reactions ^{40}Ar+^{232}Th taking from Ref. [19].

Table 2 ^{40}Ar+^{232}Th Reactions and their Different Compounds and Paramenters

Reaction	CN	x_{fiss}	E_{thresh}	B_f	Ref.
^{40}Ar+^{232}Th	^{225}Fr	0.73	47±4	6.0±0.6	[19]
^{40}Ar+^{232}Th	^{228}Ra	0.74	34±2	5.3±0.5	[19]
^{40}Ar+^{232}Th	^{228}Ra	0.74	46±6	5.9±0.3	[19]
^{40}Ar+^{232}Th	^{228}Ra	0.74	66±7	7.0±0.2	[19]
^{40}Ar+^{232}Th	^{230}Ac	0.75	18±2	4.7±0.4	[19]
^{40}Ar+^{232}Th	^{230}Ac	0.75	21±3	5.2±0.3	[19]
^{40}Ar+^{232}Th	^{230}Ac	0.75	32±4	6.2±0.2	[19]

There are three values of mean fission barrier B_f for ^{228}Ra and ^{230}Ac, respectively. We took their mean value with weight and their external errors as the following: 6.07±0.16 MeV for ^{228}Ra and 5.37±0.15 MeV for ^{230}Ac, respectively.

In general, the parameters B_f listed in Table 1 and 2 are with $\hbar\omega = 0.5 \sim 1.0$ MeV.

According to the analysis and review above, we recommended fission barrier parameters for 17 nuclei, including some ultra neutron-deficient nuclei and some short half-life radioactive ones, which could be used in nuclear data calculations and evaluations in applications on needs. The recommended parameters are listed in Table 3.

Table3 Recommended fission barrier Paramenters

CN	x_{fiss}	B_f (MeV)	$\hbar\omega$ (MeV)	Ref.
^{158}Er	0.60	11.2±2.0	0.5~1.0	[7,8]
^{168}Yb	0.60	10.4±2.4	0.5~1.0	[7,9]
^{178}W	0.64	10.3±2.3	0.5~1.0	[7,10]
^{188}Pt	0.67	7.1±1.2	0.5~1.0	[7,10]
^{188}Pb	0.72	8.2±0.6	1.0	[1~6]
^{192}Pb	0.72	6.3±0.64	0.5~1.0	[7,14]
^{196}Po	0.73	7.4±0.6	0.5~1.0	[1~6]
^{198}Pb	0.70	7.1±1.1	0.5~1.0	[7,9]
^{200}Pb	0.70	7.8±0.67	0.5~1.0	[7,9,15]
^{210}Po	0.71	8.0±0.8	0.5~1.0	[7,9]
^{213}Fr	0.74	6.2±0.6	0.5~1.0	[7,11]
^{224}Th	0.76	5.5±0.5	0.5~1.0	[7,12,17]
^{225}Fr	0.73	6.0±0.6	0.5~1.0	[19]
^{228}Ra	0.74	6.07±0.16	0.5~1.0	[19]
^{230}Ac	0.75	5.37±0.15	0.5~1.0	[19]
^{239}Np	0.78	4.3±0.1	0.5~1.0	[13]
^{251}Es	0.83	1.8±0.2	0.5~1.0	[10]

References

[1] A.N. Andreyev, D.D. Bogdanov, S. Saro, et al., Phys. Letter B 312,49-52(1993)

[2] L.G. Moretto, Proc. Symp. On Phys. And Chemi. of Fission (Rochester NY.)1973; IAEA report IAEA SM-174/204(IAEA, Vienna) p.329

[3] A.Stolory and J.A. Harvey, Phys. Rev.108, 353(1957)

[4] P. Moller and J. R. Nix, Los Alamos Preprint LA-YR-86- 3983(1986)

[5] A.N. Andreyev et al., JINR Rapid Commun. 2(53), 35(1992)

[6] A.N. Andreyev et al., Yad Fiz. 52,640(1990)

[7] M.Thoennessen and G. F. Bertsch, Phys. Rev. Letter, Vol.71, No.26, 4303(1993)

[8] A. Ganron et al., Phys. Rev. C35, 579(1987)

[9] D.J. Hinde, R. J. Xharity, G. S. Foote et al., Nucl. Phys. A452, 550(1986)

[10] J. O. Newton, D. J. Hinde, R. J. Charity et al., Nucl. Phys. A483, 126(1988)

[11] D. J. Hinde, D. Hilscher and Rossner, Nucl. Phys. A502, 497c(1989)

[12] D. Hilscher and Rossner, Ann. Phys. Fr17, 471(1992)

[13] M. Strecker, R. Wien, P. Plischke et al., Phys. Rev. C41, 2172(1990)

[14] J. P. Lestone, J.R. Leigh, J. O. Newton et al., Phys. Rev. Letter, 67, 1078(1991)

[15] R. Butsch, M. Thoennessen, D. R. Chakrabarty et al., Phys. Rev. C41, 1530(1990)

[16] I. Dioszegi, D. J. Hofman, C.P. Montoya et al., Phys. Rev. C46, 627(1992)

[17] M. Thoennessen, D. R. Chakrabarty, M.G. Herman et al., Phys. Rev. Letter, 59, 2860(1987)

[18] D.J. Hofman, B.B. Back, I. Dioszegi, et al., (to be published)

[19] E. -M. Eckert et al., Phys. Rev. Letter, 64, 2483(1990)

DPA Cross Section Calculated with UNF Code

ZHANG Jingshang

China Institute of Atomic Energy, P.O.Box 275(41) Beijing *102413*

e-mail zhangjsh@iris.ciae.ac.cn

Introduction

All of the structure nuclear materials have crystal lattice structure. The radiation damage implies the damage in varying degree in their crystal lattice structure, which is account for the changing of internal stress intensity and other properties. In general the radiation damage is measured in three fields: displacement of primary atom; production of the hole in the crystal lattice structure; and helium gas production. On the other hand, various nuclear reactions could provide amount of neutrons and gamma ray. Since their long free-path in the material the main task is radiation protection, besides the secondary reaction induced by them.

In the case of low and middle incident energies the radiation damage mainly caused by elastic scattering and inelastic scattering processes. The damage quantity is estimated by dpa.annal with the unit of b·keV. If the dpa cross sections are obtained with the unit of barn, then multiplying the current of the incident particles, then one can obtain the annual damage quantity.

The energy of the residual nuclei is depleted by three ways:

(1) The energy to get rid of the crystal lattice, which is the threshold energy of the nucleus in the crystal lattice, as the example, some effective threshold energies E_d in the unit of eV of structure materials are given in Table 1.

Table 1 Effective threshold energy of PKA in unit of eV

Material	Al	Ti, Cu	Cr,Fe,Co,Ni	Nb,Mo	W
E_d / eV	25	30	40	60	90

(2) The ionization of the electrons, which only reduce the energies of the residual nucleus, but do not affect the material damage.

(3) Displacement of primary atom in the material causes the hole production in the crystal lattice, which is the main part of the material damage. Only the kinetic energy of the residual nucleus is larger than the threshold energy of the primary knock-on atom (PKA), the displacement of primary atom could be happen.

1 Displacement of Primary Atom

The energies used for the electron ionization and displacement of primary atoms are denoted by $\eta(T)$ and $\nu(T)$, respectively. A_T and Z_T refer to the mass number and charge number of the target, respectively. The energy accumulated in the target material can be given by

$$\hat{E}(E_0) = N\int_{E_d}^{E_0}\frac{\mathrm{d}x}{\mathrm{d}E}\mathrm{d}E\int_{E_d}^{T_{max}} T[(\eta(T)+\nu(T)]\frac{\mathrm{d}\sigma}{\mathrm{d}T}\mathrm{d}T \qquad (1)$$

where T is the kinetic energy of the residual nucleus, N is the atomic density of the (1/cm^3), E_0 stands for the incident energy, $\mathrm{d}E/\mathrm{d}x$ is the stopping power of the target material, $\mathrm{d}\sigma/\mathrm{d}T$ is the spectrum of the recoil residual nucleus in laboratory system, which is related sensitively to the type of incident particle and energy.

The spectrum of the recoil residual nucleus can be calculated by UNF code with full energy balance[1], while in JENDL the effective single particle emission approximation is employed. The hole defective caused by the displacement of primary atom $\nu(T)$ can be calculated by Lindhard model[2,3]. In this model the dimensionless primary knock-on energy is defined by ε

$$\varepsilon = \frac{T(\mathrm{keV})}{0.0869\times Z_T^{7/3}} = \frac{T(\mathrm{eV})}{86.931 Z_T^{7/3}} \qquad (2)$$

The number of the displacement of primary atom caused by per PKA is given by

$$\nu(T) = \frac{1}{2E_d}\frac{T}{1+k_L g(\varepsilon)} \qquad (3)$$

Based on the study from Robinson[4], for elastic scattering of atom the number through the displacement of primary atom has the following form

$$\nu(T)=\frac{\beta T}{2E_{\mathrm{d}}} \tag{4}$$

where β=0.8 is used[3].

In Lindhard model, for a single constituent rather than an alloy in Eq.(3)

$$k_{\mathrm{L}}=0.1334Z_{\mathrm{T}}^{2/3}/A_{\mathrm{T}}^{1/2} \tag{5}$$

$$g(\varepsilon)=\varepsilon+0.40244\varepsilon^{3/4}+3.4008\varepsilon^{1/6} \tag{6}$$

For an alloy (A_1, Z_1, and A_2, Z_2), A_1, Z_1 are the mass number and charged number of recoil residual nucleus; A_2, Z_2 are that of the matrix atoms, Eq.(5) becomes

$$k_{\mathrm{L}}=\frac{(0.0793)Z_1^{2/3}Z_2^{1/2}(A_1+A_2)^{3/2}}{(Z_1^{2/3}+Z_2^{2/3})^{3/4}A_1^{3/2}A_2^{1/2}} \tag{7}$$

From the study of Robinson[4], for pure iron, chromium and nickel, the difference of calculated results from pure and alloy is only 1%.

The dpa cross section is defined by

$$\sigma_{\mathrm{dpa}}=\int_{E_{\mathrm{d}}}^{T_{\max}}\frac{\mathrm{d}\sigma}{\mathrm{d}T}\nu(T)\mathrm{d}T \tag{8}$$

The rate of displacement of primary atom is given by

$$K_{\mathrm{d}}=\sigma_{\mathrm{dpa}}\times\Phi \tag{9}$$

where Φ is the particle current, while for single atom Φ is the bombard frequency of the incident particle.

2 Calculation of DPA Cross Sections

Based on the formula mentioned above, the function to calculate the dpa cross section can be executed by UNF code. Since the energy spectrum calculated is in CMS, while in the dpa calculation of $\mathrm{d}\sigma/\mathrm{d}T$ is in LS, so the transformation from the CMS to the LS need to be performed in UNF code.

For elastic scattering process, the recoil energy of the target nucleus in CMS is obtained by

$$T_{\mathrm{el}}^{\mathrm{c}}=\frac{m_{\mathrm{n}}M_{\mathrm{T}}}{M_{\mathrm{c}}^2}E_{\mathrm{n}}, \tag{10}$$

the recoil energy of the target nucleus in LS is

$$T_{\mathrm{el}}^{\mathrm{l}}=2T_{\mathrm{el}}^{\mathrm{c}}(1-\cos\theta_{\mathrm{c}}) \tag{11}$$

where M_{n}, M_{T}, M_{c} are the masses of incident neutron, target and compound nucleus, respectively. Thus, the dpa cross section in elastic scattering channel is obtained by

$$\begin{aligned}\sigma_{\mathrm{dpa}}(el)&=\int_{E_{\mathrm{d}}}^{E_{\mathrm{c,max}}}\frac{\beta}{2E_{\mathrm{d}}}T_{\mathrm{el}}^{\mathrm{l}}\frac{\mathrm{d}\sigma}{\mathrm{d}\Omega_{\mathrm{c}}}\delta(T_{\mathrm{el}}^{\mathrm{c}}-\frac{m_{\mathrm{n}}M_{\mathrm{T}}}{M_{\mathrm{c}}^2})\mathrm{d}T_{\mathrm{el}}^{\mathrm{c}}\mathrm{d}\Omega_{\mathrm{c}}\\&=\sigma_{\mathrm{el}}(E_{\mathrm{n}})\frac{\beta}{E_{\mathrm{d}}}\frac{m_{\mathrm{n}}M_{\mathrm{T}}}{M_{\mathrm{c}}^2}(1-f_1^{\mathrm{el}}(\mathrm{c}))E_{\mathrm{n}},\end{aligned} \tag{12}$$

where $f_1^{\mathrm{el}}(\mathrm{c})$ is the Legendre coefficient of the elastic scattering angular distribution with the partial wave l=1 in CMS.

For the first particle emission from compound nucleus to discrete levels, the recoil nucleus has definite energy in CMS.

$$E_k^{\mathrm{c}}(M_1)=\frac{m_1}{M_{\mathrm{c}}}(E^*-B_1-E_{k_1}), \tag{13}$$

where m_1 ,M_1 are the masses of the first emitted particle and its residual nucleus; B_1 is the binding energy of m_1 in the compound nucleus; E_{k_1} is the level energy of residual nucleus. The energy of M_1 in LS reads[1]

$$\begin{aligned}E_k^{l}(M_1)&=\frac{m_{\mathrm{n}}M_1}{M_{\mathrm{c}}^2}E_{\mathrm{n}}+E_k^{\mathrm{c}}(M_1)_{\mathrm{c}}\\&+\frac{2}{M_{\mathrm{c}}}\sqrt{m_{\mathrm{n}}M_1E_{\mathrm{n}}E_k^{\mathrm{c}}(M_1)}\cos\theta\end{aligned} \tag{14}$$

where θ_{c} is the outgoing angle of recoil residual nucleus M_1 in CMS. Averaged by the angular distribution of recoil residual nucleus M_1, the dpa cross section has the form as

$$\begin{aligned}\sigma_{\mathrm{dpa}}(M_1)_k&=\int_{E_{\mathrm{d}}}^{E_{l,\max}}\frac{\mathrm{d}\sigma}{\mathrm{d}E_k^{\mathrm{l}}}\nu(E_k^{\mathrm{l}})\mathrm{d}E_k^{\mathrm{l}}\\&=\int\mathrm{d}\Omega_{M_1}^{\mathrm{c}}\frac{\mathrm{d}\sigma}{\mathrm{d}\Omega_{M_1}^{\mathrm{c}}}\nu(E_k^{\mathrm{l}}(M_1))\end{aligned} \tag{15}$$

In the case of continuum final states, including the emissions from compound nucleus to continuum states or the sequential multi-particle emissions. The double-differential cross section is represented in the Legendre expansion form in CMS

$$\frac{\mathrm{d}^2\sigma}{\mathrm{d}\varepsilon^{\mathrm{c}}\mathrm{d}\Omega^{\mathrm{c}}}=\frac{\sigma}{4\pi}\sum_l(2l+1)f_l^{\mathrm{c}}(\varepsilon^{\mathrm{c}})\mathrm{P}_l(\cos\theta^{\mathrm{c}}) \tag{16}$$

The dpa cross section of the recoil nucleus with the mass M_2 can be obtained by

$$\begin{aligned}\sigma_{\mathrm{dpa}}&=\int_{E_{\mathrm{d}}}^{E_{l,\max}}\frac{\mathrm{d}\sigma}{\mathrm{d}E^{\mathrm{l}}}\nu(E^{\mathrm{l}})\mathrm{d}E^{\mathrm{l}}=\int\int\frac{\mathrm{d}^2\sigma}{\mathrm{d}E^{\mathrm{l}}\mathrm{d}\Omega^{\mathrm{l}}}\nu(E^{\mathrm{l}})\mathrm{d}E^{\mathrm{l}}\mathrm{d}\Omega^{\mathrm{l}}\\&=\int\int\frac{\mathrm{d}^2\sigma}{\mathrm{d}E^{\mathrm{c}}\mathrm{d}\Omega^{\mathrm{c}}}\nu(E^{\mathrm{l}})\mathrm{d}E^{\mathrm{c}}\mathrm{d}\Omega^{\mathrm{c}}\end{aligned} \tag{17}$$

where

$$E^{l} = E^{c}(1+2\gamma\cos\theta_{c}+\gamma^{2}) \quad (18)$$

and

$$\gamma = \frac{\sqrt{m_{n}M_{2}}}{M_{c}}\sqrt{\frac{E_{n}}{E^{c}}} \quad (19)$$

The relation $E^{l} \geq E_{d}$ must be held in the Eq.(17).

As an example, the calculations of dpa cross sections of n+^{56}Fe have been performed with UNF code. Since the resonance region is below 0.8 MeV, so the model calculation only performed at the energies from 1 MeV to 20 MeV. The dpa cross section caused by gamma ray emissions is small enough to be neglected. The comparison of the calculated result and measured data is shown in Fig.1 for the total dpa cross section. The calculations indicate that elastic scattering channel is the dominant term. Therefore, the key point is to fit the measured elastic scattering data well on the cross section and angular distribution as far as possible in the model calculation. The dpa cross sections of elastic scattering channel have very different values from different evaluated neutron data files. The calculated dpa cross section with the related evaluated data in eq.(12) taken from ENDF/B-6, Jendl-3.2 and CENDL-2 from E_n=1 MeV to 20 MeV are shown in Table 2. From this table one can see that the results are very different from each other.

The sequential multi-particle emission processes give relative large recoil effect to the single particle emission. Meanwhile, the heavier emitted particle yields stronger recoil effect. Of course, dpa cross sections are also proportionally dependent on the reaction cross sections.

Table 2 The dpa cross sections of elastic scattering calculated with the data from ENDF/B-6, JENDL-3.2 and CENDL-2 at E_n=1 to 20 MeV

E_n / MeV	CENDL-2	JENDL-3.2	ENDF/B-6
1.0	657.2	633.6	491.0
3.0	1272.7	1282.0	1236.7
5.0	1146.4	1168.2	1061.0
7.0	1040.4	1033.9	980.7
9.0	910.5	945.4	996.6
11.0	883.4	969.3	1044.4
13.0	919.1	1033.0	1099.5
15.0	1011.0	1116.1	1396.5
17.0	1087.2	1188.8	990.3
20.0	1283.7	1283.1	1165.5

The dpa cross sections calculated by UNF code are listed in Table 3. The dpa cross sections induced by ^{3}He and triton emissions are not included due to very small.

Table 3 The dpa cross sections of each reaction channel and the total dpa cross section calculated by UNF code

E	in-el	n,p	n,α	n,d	n,2n
1.0	0.	0.024	0	0	0
2.02	403.4	9.85	0	0	0
4.0	719.3	251.9	1.19	0	0
6.5	746.7	714.9	70.4	0	0
8.0	750.9	631.0	166.3	0	0
10.	685.1	433.9	136.1	1.31	0
12.	561.2	189.3	63.0	6.90	0
14.	514.9	40.7	22.1	7.62	.014
16.	596.4	24.4	8.0	5.05	12.7
18.	682.8	17.5	3.32	3.18	54.7
20.	760.7	13.7	1.64	2.06	100.9

E	n,np	n,nα	n,2p	elas.	Total
1.0	0	0	0	620.2	620.2
2.02	0	0	0	626.4	1040.
4.0	0	0	0	653.9	1632.
6.5	0	0	0	694.7	2231.
8.0	0	0	0	749.1	2297.
10.	0	0	0	1089.	2344.
12.	50.0	0	0.43	1697.	2568.
14.	285.6	0.62	3.70	1961.	2836.
16.	484.3	29.6	14.5	1848.	3023.
18.	570.9	149.2	38.9	1641	3160.
20.	578.5	296.3	62.9	1384.	3200.

The results indicate that the radiation damage mainly caused by elastic scattering and inelastic scattering processes. Meanwhile, the sequential particle emissions from (n,np) and (n,nα) channels give large contribution to the dpa cross section due to large reaction cross sections at high energies.

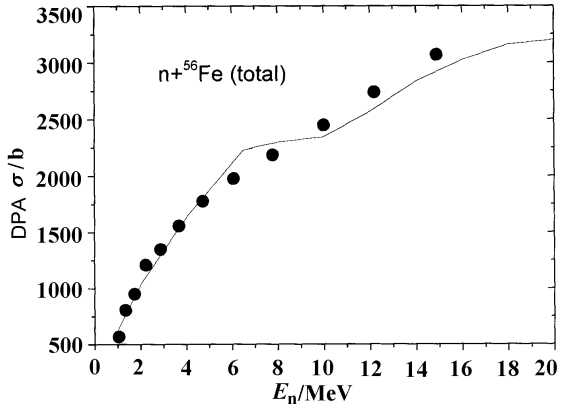

Fig.1 The total dpa cross section of n+^{56}Fe calculated by UNF code. The data are taken from Ref. [5]

Reference

[1] ZHANG Jingshang. Commou. Nucl. Data. CNIC-01475 CNDC-0027 INDC(CPR)0050/L 23,18 (2000)
[2] J. Lindhard et al., Mat. Pys. Medd. Dan. Vid. Selsk., 33, 10 (1963)
[3] D. G. Doran, Nucl. Sci. Eng., 49,130,(1972)
[4] M. T. Robinson, Phil. Mag., 17, 639 (1968)
[5] D. G. Doran and N. J. Graves, HEDL-TME 7670, Hanford Engineering Development Laroratory, 1976

The Production and Transmission of Covarience in the Evaluation Processing of Fission Yield Data

LIU Tingjin
China Nuclear Data Center, CIAE, P.O.box 275(41) Beijing, 102413
e-mail tjliu@iris.ciae.ac.cn

【abstract】 *The production and transmission of correlation in the evaluation processing of fission yield data, including average with weight, ratio and sum consistence adjusting, are researched. The variation of the averaged and adjusted yields and/or rations with the correlation coefficient of the input data are investigated. The results obtained are reasonable in physics.*

Introduction

The error, as traditionally given, is only the diagonal elements of the covariance matrix and only describes the total error of the data, nothing about the systematical error or the correlation of the data. The systematical error is more important for the engineering applications, because the statistical one can be counteracted in the calculation by using large amount of data, but the systematical one could not be. For evaluators and experimenters, the information is given completely, only in the case of the covariance matrix is given out.

As well known that the correlation describes the systematical error or medium and long range error[1] in the experiment, for example, due to calibration of detector efficiency, multiple scattering correction and measurement geometry, sample quantification, normalization etc. All of these depend on the experimental conditions. Also the correlation can be produced in the data evaluation processing, which is not only from the mathematical restriction condition, for example, the curve must be smooth in the curve fitting by using least-square method, but also from physical restrictive condition, for instance, the total must be the sum of all partials, absolute cross section or fission yield should be consistent with their concerned ratios measured etc.

For fission yield data, the main processing in the evaluation is

a. average with weight;

b. the consistency adjusting between the absolutely measured yields and the ratios concerned;

c. the consistency adjusting between the sum and its partials, e.g. cumulative yield and its independent yields concerned.

All of these processing can be done by using code ZOTT[2], with the different form of the sensitivity matrix. ZOTT is a general partitioned least squares method code, using for adjusting a combined set of data $Y(I)$ of differential and integral quantities with covariance $CY(I,J)$ to new values $Y'(I)$ with covariance $CY'(I,J)$, which are minimum variance linear unbiased estimator of the true values and satisfy the physical relationship prescribed by the sensitivity matrix $S(K,L)$, where I or J is the total number of differential plus integral quantities, K is the number of the integral quantities and L is the number of differential quantities.

In this paper, the production and transmission of the covariance in the fission yield data evaluation processing, as listed above, are investigated. The first section is for the average with weight, and the second one is for ratio adjusting, the third one is for sum adjusting, a practical example is given in the section

4 and the conclusion remarks are given in section 5 at the last.

1 Averaging with Weight

The data measured at same energy point for the same quantity should be averaged with weight, which can be done with code AVERAG [3] or ZOTT. The former is a special code for averaging, weighted or mathematical average. In the later case, the sensitivity matrix should be defined, as given below.

An example is given for the fission yield of product nuclide ^{103}Ru at thermal energy point. There are 7 sets of absolutely measured data. In this case, the sensitivity matrix is given in the form of (6 rows × 1 column), which means the all of last 6 quantities should be equal to the first one, that is the result should be the average with weight of all 7 quantities.

The calculated results with different correlation coefficients are given in Fig. 1. When the correlation coefficient is 0.0, the results, including the quantity itself and its error, are the same as calculated with code AVERAG. It means that the adjusted value is the mean with weight and its error is the internal error of the mean with weight, only depends on the fission yield error D$Y(I)$, no matter how much the differences among the yields $Y(I)$ are. From Fig.1 it can be seen that the mean increases with the increasing of correlation coefficient ρ. When correlation coefficient ρ varies from 0.0 to 0.999, the mean of the yield varies from 3.043 to 3.0656, that is 0.7% change. The change of the mean error is shown in Fig. 2. It can be seen that when the correlation increases, the error of the mean increases slightly from 0.0299(0.98%) to 0.0373(1.22%) at first, then decreases rapidly and very sharply to 0.0 when the correlation coefficient closes to 1.0 at last.

2 Ratio Adjusting

It is the general case that not only the yields themselves but also their ratios were measured. Both kinds of data are valuable and should be used in the fission yield data evaluation, especially the ratio, which was measured with high accuracy. Due to the measurements could be done at different laboratories and different time, the yields and their ratios are often not consistent with each other. It is the task of the evaluation to get a set of fission yield data, the variance of which and their ratio to the corresponding experimental data are minimum. This can be done by using code ZOTT, taking the form of sensitivity matrix as shown in following example.

There are lot of measured data for ^{140}Ba yield, 9 set of data for the yields at thermal energy (Y_t), 3 sets of data at fission spectrum (Y_f), 2 sets data around 14 MeV (Y_h), and 2 sets data for the ratios of the yield at fission spectrum over the yield at thermal ($R_{f/t}$), 1 set for the ratio of around 14 MeV over thermal($R_{h/t}$). To simplify the processing with code ZOTT, they were averaged with code AVERAG (the same result with ZOTT as discussed above) for the yields at thermal, fission spectrum, around 14 MeV and ratios of fission over thermal. As results, 3 yields at each energy point and 2 ratios and their errors were got. It was supposed that there is no correlation among the absolutely measured yields and their ratios and between two ratios, but there is correlation among the absolutely measured yields. The sensitivity matrix of this example for ratio adjusting is $\begin{pmatrix} -1 & 1 & 0 \\ -1 & 0 & 1 \end{pmatrix}$ where "-1" in the matrix means at denominator, and "1"means at numerator, so the first row, corresponding to the first ratio in the combined vector, in the matrix means the second yield over first one, that is the yield at fission spectrum over the yield at the thermal one. In the same sense, the second row means the yield around 14 MeV over the yield at thermal.

The variation of adjusted yields ratios and their errors with correlation coefficient were calculated. The corresponding ratios of the adjusted ones over the input ones are given in Fig. 3 and 4 respectively. It can be seen that the $Y_1(Y_t)$, $Y_3(Y_h)$, which were adjusted smaller to make consistence with the measured ratios, increases with the correlation coefficient increasing, and opposite $Y_2(Y_f)$, which was adjusted larger, decreases. As a result they were made closer when the correlation becomes stronger. This is reasonable in physics. As regards to the ratios, they change only as the comprehensive results of Y_2/Y_1, Y_3/Y_1 due to no correlation between them were supposed. It can be seen from Fig. 4 that all errors are smaller than input ones, especially for the ratios $R_{1/2,}$ $R_{1/3,}$ this is the statistically processing result. When the correlation increases, the error of all yields Y_1, Y_2, Y_3 increases a little at first, and then decreases, the only difference is decreasing faster for Y_1. The error of all two ratios decreases a lot with correlation increasing.

The correlation matrices of the adjusted quantities were investigated. In the case of the input data ρ=0.0, there is no correlation for the input data, the correlation of the adjusted values was completely induced in the processing due to the restrict condition of ratios. Also the correlation between $Y_{2,}$ Y_1 and R_1 as well as $Y_{3,}$ Y_1 and R_2, is quite large. The other elements are quite small, due to the correlation among them was only induced indirectly. When the correlation coefficient ρ=0.9 of the input data, the correlation among the adjusted quantities is quite strong, not only among the yields themselves Y_1, Y_2, Y_3, which was transferred from the input data

correlation, but also between the ratios R_1, R_2 and between yield and ratios, which was induced in the processing through the ratios. As an example, in Fig. 5 is given the correlation between yield Y_1 and yields Y_1~Y_3, Ratios R_1, R_2.

3 Sum Adjusting

In the fission yield evaluation processing, sometimes it is needed to make the sum of some quantities equal a value. For example, the sum of independent yields in a decay chain equals its chain yield, the chain yield sum of all mass number equals 2.0 etc. This can also be done by using code ZOTT, taking the sensitivity matrix in the form as given in the following example.

Taking the mass chain A=99 as an example, there are fission product nuclides $_{35}$Br, $_{36}$Kr, $_{37}$Rb, $_{38}$Sr, $_{39}$Y, $_{40}$Zr, $_{41}{}^{m}$Nb, $_{41}$Nb, $_{42}$Mo. Among them, the independent yields of the first three are very small ($<10^{-5}$), the independent yields of other 6 are 0.133158, 1.94933, 3.58394, 0.406579, 0.0299649, 0.0428140 respectively, but the recommended value based on the measured data of cumulative yield for ^{99}Mo is 6.15000, they are not consistent with their sum and should be adjusted. For this, the sensitivity matrix was constructed as only one low, and all of the 6 elements are 1. That means the sum of first 6 quantities should be equal to the seventh one. In this example, the correlation coefficient was changed from 0.0 to 0.999 in the calculation to study the effect of the correlation on the sum adjusting result.

The variation of the yields with correlation coefficient was calculated. The ratio of adjusted yields over input ones is given in Fig. 6 as a function of correlation coefficient. It can be seen that the adjusting for the yield is very small, the maximum one is 0.1% for Y_3, whose error is the largest one in the input data. This is because there is no large discrepancy in the input data. Another feature can be seen from Fig. 6 is that the adjusting increases with increasing the correlation for all yields but Y_3, whose adjusting decreases. The stronger correlation makes them stronger influence with each other, as a result, the yields with smaller errors were also adjusted a little more.

The errors of the adjusted values were also calculated. The variation of their ratio of the adjusted one over the input one is shown in Fig. 7. It can be seen that the ratios of all yield errors decrease in a similar way from 1.0 to closing 0.0 with the correlation coefficient increasing from 0.0 to 0.999, except for the ratio of yield Y_3, whose input error is relatively large, so it was adjusted more (see Fig. 6) and its error was reduced a lot (about 80%) even in the case of the correlation coefficient is 0.0, as a result, even the correlation become stronger, it only can be reduced more slowly.

The correlation matrices of the adjusted yields were studied for correlation coefficient ρ of input data from 0.0 to 0.999. It can be seen that the correlation is not large when the input correlation is small, even the correlation coefficients ρ=0.9 of the input yields, the ones of the adjusted yields are about 0.4~0.5, which is much smaller than the input one. Another feature of the matrices is that the correlation between the yield Y_3 and Y_1, Y_2, Y_4~Y_6 is negative and the correlation between the sum yield Y_7 and other 6 yields Y_1~Y_6 is positive, except for the case of input ρ=0.9, where the correlation of the input data is quite strong. These are reasonable in physics. Increasing of any one from the partial yields Y_1~Y_6 should make the increasing of the sum yield Y_7. Keeping the sum yield Y_7 unchanged, increasing of some partial yields, the others should decrease, for this example all of partial yields change in the same direction, but Y_3, whose error of the input data is quite large comparing to others, in opposite direction. In Fig.8 is shown the variation of the correlation coefficients of yield Y_1 with Y_1~Y_7. It can be seen that all of them increase with the increasing of the input correlation coefficient ρ(c in the Fig.), except for ρ_{13}, which is decreases.

4 Practical Example

In the following a practical example is given to show how to get the input covariance matrix and how the covariance is transferred and produced in the practical fission yield data evaluation.

For the yields of fission products ^{147,149,151,152}Sm at thermal energy, there are 5 sets of measured data for yields themselves and their ratios. All of them were measured with mass spectroscopy method absolutely or relatively. They are listed in Table 1. The quantities were measured for each isotope is listed in Table 2.

Table 2 The measured quantities for each product nuclides

Number	Nuclide	Yield Y	Ratio R
1	^{147}Sm	Ref. [1], [2]	Ref. [4]
2	^{151}Sm	Ref. [1], [2]	Ref. [4]
3	^{152}Sm	Ref. [1], [2]	Ref. [4], [5]
4	^{149}Sm	Ref. [1], [3]	

Based on the total and systematical error given in the Table 1 for each reference and the measured quantities for each product listed in Table 2, the input data and their covariance matrix were constructed. There are all together 12 quantities in the input vector, including 2 sets of yield data for each product, 4 sets

Table 1 Measured data for the fission yields of ^{147,149,151,152}Sm at thermal energy

Ref.	EXFOR	Method (Year)	Error given	Error adjusted	Syst.Error estimated	Note
1	13270003	Mass (1970), Absolutely	⩽1.0%	1.5%, (10% discre. with ^{152}Sm)	0.9%	1)
2	13384005	Mass (1955), Relatively (^{149}Sm)	No	2.0%	1.7%	2)
3	13386002	Mass (1955), Absolutely	No	3.0%	1.7%	1)
4	13384006	Mass (1955), Relatively (^{149}Sm)	No	1.5% (Ratio)	1.3%	3)
5	13352003	Mass (1950), Relatively (^{149}Sm)	No	1.5% (Ratio)	1.3%	3)

Note: 1) The fission rate, which is the main source of the systematical error, was measured also by mass spectroscopy method. The contribution to the total error is about 1/3, so the systematical error is $(1.5^2\times1/3)^{1/2}$=0.9.

2) The error mainly comes from the standard of ^{149}Sm, about 70%.

3) Only the ratio was used, which was calculated from fission yield divided by the yield of the standard ^{149}Sm. The error mainly comes from the standard of ^{149}Sm, about 70%.

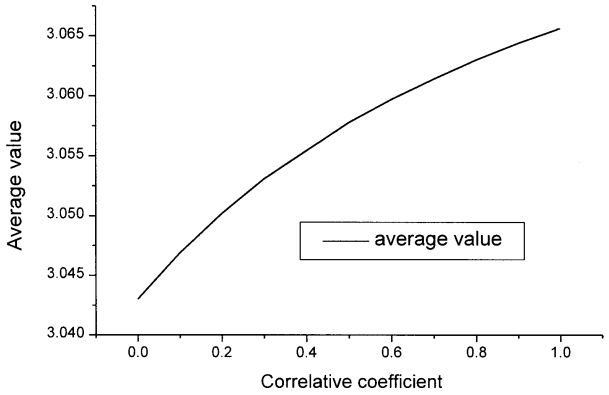

Fig. 1 The variation of the mean with the correlation coefficient

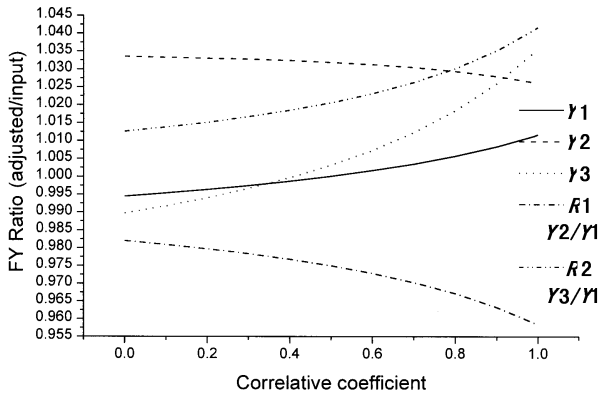

Fig. 3 The variation of the adjusted yields and ratios with the coefficient in the ratio adjusting

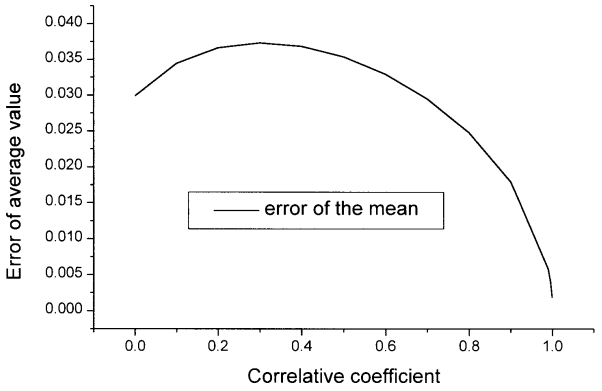

Fig. 2 The variation of the mean error with the correlation coefficient

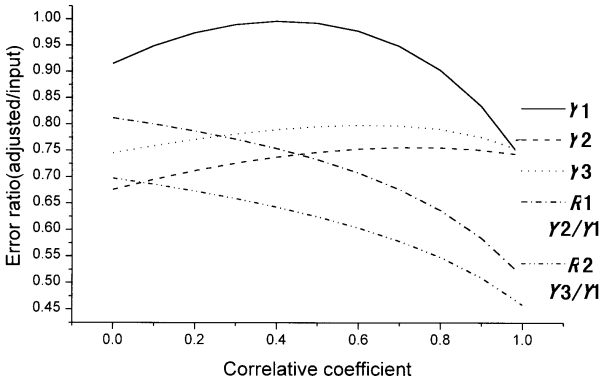

Fig. 4 The variation of the error of the adjusted yields and ratios with the correlation coefficient in the ratio adjusting

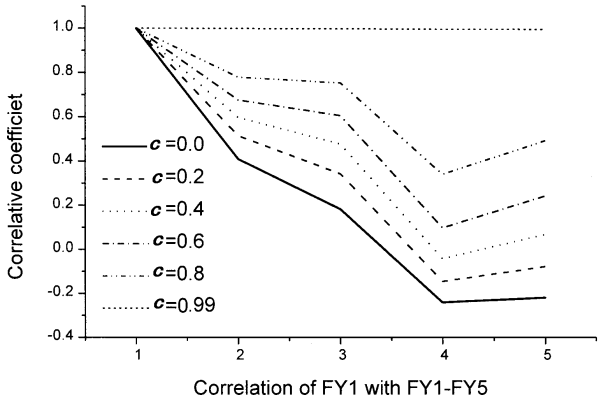

Fig. 5 The variation of the correlation coefficient between the Y_1 and $Y_{1\sim3}$, $R_{1,2}$ with the input correlation coefficient in the ratio adjusting

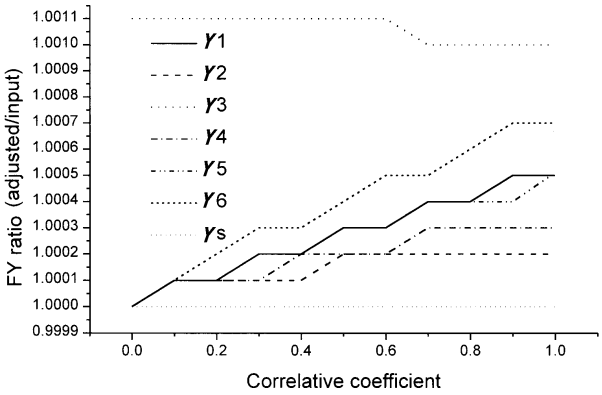

Fig. 6 The variation of the adjusted yields with the input correlation coefficient in the sum adjusting

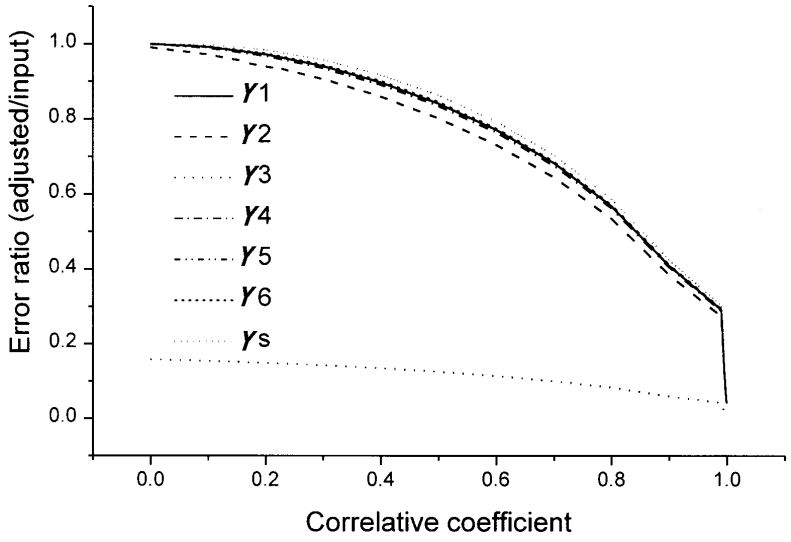

Fig. 7 The variation of the error of adjusted yields with the input correlation coefficient in the sum adjusting

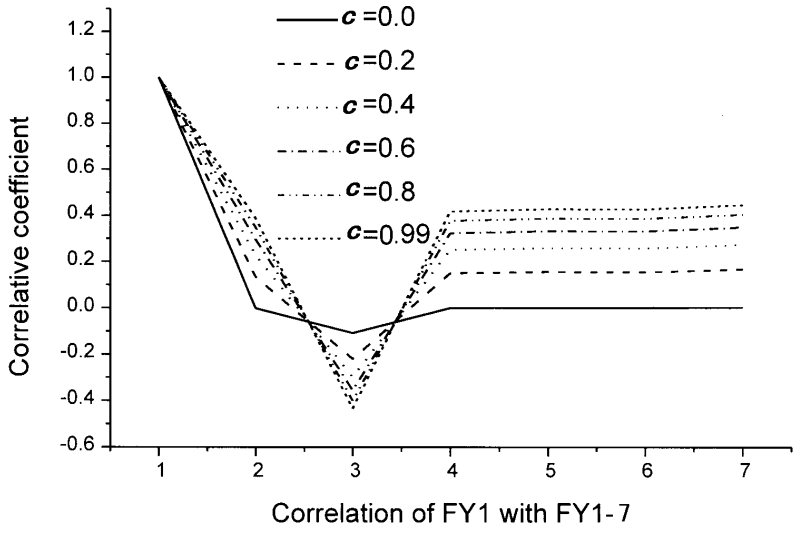

Fig. 8 The variation of the correlation coefficient between Y_1 and $Y_{1\sim7}$ with the input correlation coefficient in the sum adjusting

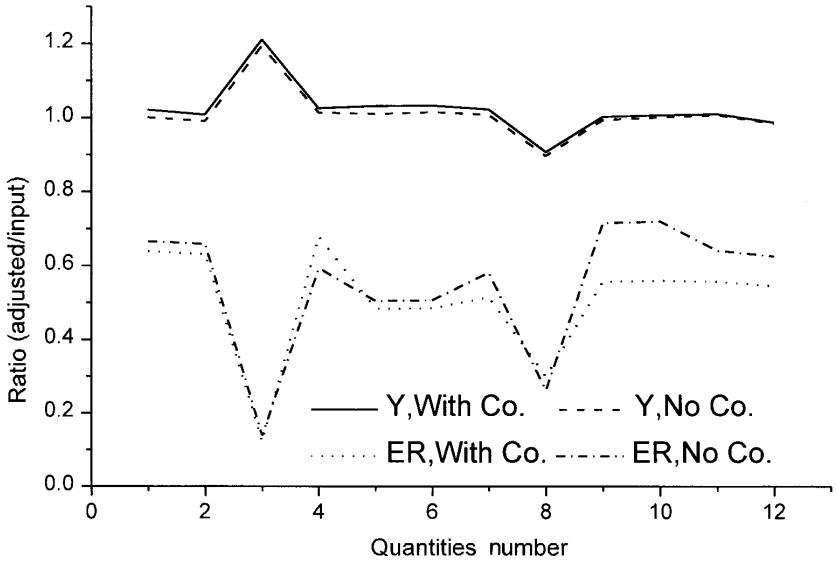

Fig. 9 Comparing between the adjusted data with and without correlation for ^{147,151,152,149}Sm yield data and their errors

of ratio data. The relationships among them were defined by the sensitivity matrix, which is somewhat complicated.

processing results (the ratio over the input data) are given in Fig.9 with the comparing to the one without correlation. The following features can be seen from the figure:

1) All of the quantities, including yields themselves and their ratios, were changed a little, except for the third one (the first yield of ^{152}Sm), and the 8-th (the second yield of ^{149}Sm), both were adjusted about +20% and –10% respectively, for they have larger error of the input data

2) All of the quantities, including yield themselves and their ratios, adjusted somewhat larger with correlation than without.

3) The errors of all quantities were reduced to about 50% comparing to input ones, except to about 10% for Y_3, and about 30% for Y_8, the errors of both input dada are relatively larger, as discussed above.

4) There are no large differences between the errors of all quantities adjusted with and without correlation, although they are a little lower with correlation than without correlation.

5 Conclusion Remarks

From above working over, the following can be concluded:

1) The code ZOTT can be used for the commonly evaluation processing of the fission yield data, including average with weight, ratio adjusting and sum adjusting, just taking the different form of the sensitivity no matter the data have or not have correlation;

2) The correlation of the evaluated fission yield data (also other nuclear data) can be produced in the data evaluation processing, which depends on the processing method, as a result, the processed data have the correlation, even though the input data have no correlation (the non-diagonal elements of the covariance matrix are zero);

3) The correlation of the input data, which depends on the experimental conditions, can be transmitted in the data evaluation processing, like the error propagation in the traditional data processing;

4) The variations of the adjusted yields, ratios and their errors with the correlation coefficient, either in the case of average, ratio adjusting or sum adjusting, are reasonable in physics, although some of them are difficult to be imaged and explained directly.

Reference

[1] V. McLane, C. L. Dunford and P. F. Rose, ENDF-102, BNL-NCS-44945(1995)

[2] D. W. Muir Nucl. Scie. And Eng., 101,88(1989)

[3] LIU Tingjin, CNDP, 19, 103(1998)

Transition Analysis of Ne-like Ge XXIII

CHEN Huazhong

Nuclear Physics Department, China Institute of Atomic energy, P.O.Box 275(80) Beijing 102413

【abstract】*Transition between fine-structure levels arising from the $2p^5 3s$, $2p^5 3p$ and $2p^5 3d$ configurations of highly charged Ne-like ions, obtained from GRASP (General-purpose Relativistic Atomic Structure Program) calculations, are tabulated for Ge XXIII.*

Introduction

Over the past 15 years, substantial efforts have been directed towards understanding the lasing possibilities for certain $2p^5 3s$--$2p^5 3p$ transitions in Ne-like ions. Significant progress has been made during this period and an overview of the results has been provided by Nilsen and Scofield[1]. Transition between fine-structure levels arising from the $2p^5 3s$, $1s^2 2s^2 2p^5 3p$ and $2p^5 3d$ configurations of highly charged Ne-like ions have recently attracted large interest in connection with attempts to achieve amplification of radiation at short wavelengths [2,3]. They also have a considerable astrophysical interest, as they can be used for diagnostic purposes in high-temperature plasmas [4,5]. Identification of the spectra of all these above mentioned systems is practically impossible without corresponding theoretical analysis. In this situation, accurate theoretical wavelength predictions can be of great value.

In this work, transition wavelengths of Ne-like Ge XXIII are calculated by means of GRASP code[6]. Theoretical calculation can provide transition wavelengths, energy level lifetimes and so on for experimentation . Such calculations could be done prior to the corresponding experimental observations or after them to help to explain the interesting phenomena found in experimental analyzing. GRASP presented by I.P. Grant[7] extends the previously published program which solved the atomic orbital wavefunctions and energy levels. Two types of the charge distribution (point charge distribution and Fermi two-parameter distribution) in nucleus were adopted to calculate wavelengths of highly stripped ions. Making use of GRASP one can be in a position to perform calculations of the energy spectra, transition probabilities of all atoms of the Periodical Table and ions of any ionization degree.

1 Theory

Relativistic atomic structure theory is ultimately based on quantum electro-dynamics. The GRASP approximation for the calculation of atomic stationary states and transitions among them has been described in the literature [8~10]. Only a brief outline of the theory is given in this paper.

From the theoretical point of view the atom is considered to be a many-body system. As described more fully in Ref.[11] we construct atomic state functions (ASF) from a linear combination of configuration state functions (CSF) which are eigenfunctions of J^2,J_z and parity. These in turn are built from single-electron Dirac equation.

All the dominant interactions in the highly stripped ions are included in the Dirac-Coulomb Hamiltonian,

$$\hat{\mathrm{H}}^{\mathrm{DC}} = \sum_{i=1}^{N} \hat{\mathrm{H}}_i + \sum_{i=1}^{N-1} \sum_{j=i+1}^{N} \left| \hat{r}_i - \hat{r}_j \right|^{-1} \tag{1}$$

in the first term (in atomic units) ,

$$\hat{\mathrm{H}}_{\hat{i}} = c \sum_{j=1}^{3} \alpha_j p_j + (\beta - 1)c^2 + V_{\mathrm{nuc}}(r), \tag{2}$$

is the one-body contribution for an electron due to its kinetic energy and interaction with the nucleus—the rest energy; c^2, has been subtracted out; r is the position vector of the electron; c is the velocity of light; $p \equiv -\mathrm{i}\nabla$ is the momentum operator. The nuclear potential energy, $V_{\mathrm{nuc}}(r)$, takes the two types of the charge distribution in nucleus. First, takes the Coulomb form or point charge distribution in nucleus, $V_{\mathrm{nuc}} = -Z/r$ (where Z denotes the atomic number of the system). Second, takes the Fermi two-parameter distribution,

$$\rho_{nuc}(r) = \frac{\rho_0}{1 + \mathrm{e}^{(r-c1)/a}}, t = (4 \ln 3)a \tag{3}$$

the parameter c1 is the "half-charge radius", the value of r for which $\rho_{nuc}(r)=0.5\rho_0$; it thus provides a measure of the nuclear radius. The surface thickness t, which measures the distance over which the density falls from 0.9 ρ_0 to 0.1 ρ_0. For A (nuclear numbers of system)＞12 , there is a central region of fairly uniform charge density given by $\rho_0=0.17\ fm^{-3}$, α=0.54 fm[12]. The nuclear potential can be calculated from the identity[7]

$$-rV_{nuc}(r)=4\pi(\int_0^r \rho(s)s^2 ds + r\int_r^\infty \rho(s)s ds)$$

2 Results

From the paper[13] we know that GRASP is an available program for researching the atomic structure. Wavelengths of highly ionized atoms Ne-like Ge XXIII are computed by means of GRASP code with two types of the charge distribution in nucleus. Table 1 give out the comparison of transition wavelengths between theoretical calculation performed by this work and experimental data taken from experimentation performed in the Department of Nuclear Physics of the China Institute of Atomic Energy (CIAE)[14,15]. From Table 1 we can see that seven new 3s—3p transition experimental values in Ge XXIII have been obtained by CIAE group. In Table 1, Model 1 for point charge distribution in nucleus, Model 2 for Fermi two-parameter distribution in nucleus.

From these comparisons we can see that there are differences of wavelengths between theory and experiment for highly ionized atoms Ne-like Ge XXIII, but no differences or small differences of wavelengths between theoretical calculations with two types of the charge distribution in nucleus. In this work, the main differences come from correlation effects not being considered completely. We will improve the GRASP code to include more correlation effects completely in the future.

Table 1 Wavelength comparison between calculated & measured data for Germanium XXIII (Ge^{22+})

Transition	Wavelength(in Å [2])		
	Exp.(CIAE)	Model 1	Model 2
$3p(3/2,1/2)_1$----$3d(3/2,3/2)_2$	179.73[1]	179.06	179.06
$3p(1/2,1/2)_1$----$3d(1/2,3/2)_2$	186.71[1]	186.83	186.83
$3p(1/2,3/2)_1$----$3d(1/2,5/2)_2$	206.54[1]	206.78	206.78
$3p(3/2,3/2)_3$----$3d(3/2,5/2)_4$	209.08[1]	209.27	209.27
$3s(3/2,1/2)_2$----$3p(3/2,3/2)_2$	221.32[1]	221.53	221.55
$3s(3/2,1/2)_3$----$3p(3/2,3/2)_3$	238.36	238.22	238.24
$3s(3/2,1/2)_2$----$3p(3/2,1/2)_2$	269.94[1]	269.68	269.71
$3s(3/2,1/2)_1$----$3p(3/2,1/2)_2$	286.43[1]	286.86	286.88

1) measured data are published first time in the world; 2) 1Å=10^{-10}m.

Reference

[1] Nilsen J and Scofield J H 1994 Phys. Scr. **49** 588-91
[2] Rosen, M.D.et al. Phys. Rev. Lett. 54.106 (1985)
[3] Matthews, D. L. et al. Phys. Rev. Lett. 110 (1985)
[4] Jupen, C., Mon.Not.R.astr. Soc. 208, 1P (1984)
[5] Feldman, U., Doschek, G. A. And Seely, J. F. Mon.Not.R.astr. Soc. 212, 41P (1985)
[6] Dvall K. G et al. Comput. Phys. Commun. 55(1989)425
[7] Grant I. P. et al. Comput. Phys. Commun. 21(1980)207
[8] I.P.Grant Advan. Phys. 19(1970)747
[9] I.P.Grant, J.Phys. B7(1974)1458
[10] I.P.Grant, in; Methods in Computational Chemistry, Vol, 2, Relativistic Effects in Atoms and Molecules, ed. S. Wilson (Plenum, New York, 1988) p.1
[11] I.P.Grant and B.J.Mchenzie, J. Phys. B13 (1980) 1671
[12] J.M.Irvine, Nuclear structure theory, (Pergamon Press,Oxford, 1972)
[13] CHEN Huazhong, Commu. of Nucl. Data Progress, 138,145(1999)
[14] C.Jupen, et al. Physica Scripta, Vol. 61, 443(2000)
[15] X.T.Zeng, et al. Physica Scripta, Vol. 61, 464(2000)

CINDA INDEX

Nuclide	Quantity	Energy/ eV		Lab	Type	Documentation				Author, Comments
		Min	Max			Ref	Vol	Page	Date	
^{71}Ga	(n,γ)	2.5-3		AEP	Expt	Jour CNDP	26	6	Dec 2001	HUANG Xiaolong +, SIG
^{94}Za	(n,γ)	2.5-3		AEP	Expt	Jour CNDP	26	6	Dec 2001	HUANG Xiaolong +, SIG
^{114}Cd	(n,2n)	1.5+7		LNZ	Expt	Jour CNDP	26	5	Dec 2001	ZHU Xuebin +, SIG
^{174}Hf	(n, γ)	1.6+5	1.2+6	SIU	Expt	Jour CNDP	26	1	Dec 2001	XIA Yijun +, SIG
^{191}Ir	(n,γ)	2.5-3		AEP	Expt	Jour CNDP	26	6	Dec 2001	HUANG Xiaolong +, SIG
^{204}Pb	Evaluation	1.0-5	2.0+7	SIU	Eval	Jour CNDP	26	10	Dec 2001	MA Gonggui, SIG, DA, DA/DE
^{207}Pb	Evaluation	1.0-5	2.0+7	SIU	Eval	Jour CNDP	26	10	Dec 2001	MA Gonggui, SIG, DA, DA/DE
^{235}U	Fission Yield	1.9+7		AEP	Expt	Jour CNDP	26	8	Dec 2001	BAO Jie+, Fission Yield
^{238}U	Fission Yield	2.2+7		AEP	Expt	Jour CNDP	26	2	Dec 2001	LIU Yonghui+, Fission Yield

中国核科技报告 CNIC－01630，CNDC－0031，INDC（CPR）－056/L
《Communication of Nuclear Data Progress》. No. 26 / 刘廷进等著. －北京：中国核工业音像出版社，2001. 12
出版批文号：新出音管 [2001]451 号
国际标准书号：ISBN 7-89998-074-7/TL·001

中国核工业音像出版社出版发行
责任编辑：李曼莉
社址：北京市海淀区阜成路 43 号 邮政编码：100037
中国核科技报告编辑部排版
A4 开本 印张 2 字数 90 千字
2001 年 12 月北京第一版
印数 1－500